Recent Advances, Open Questions and Future Directions in Solar-Terrestrial Research

I. A. Daglis[1], W. Baumjohann[2], J. Geiss[3], S. Orsini[4], E. T. Sarris[5], M. Scholer[2], B. T. Tsurutani[6], and D. Vassiliadis[7]

[1]Institute of Ionospheric and Space Research, National Observatory of Athens, 15236 Penteli, Greece
[2]Max-Planck-Institut für extraterrestrische Physik, 85740 Garching, Germany
[3]International Space Science Institute, 3012 Bern, Switzerland
[4]Istituto di Fisica dello Spazio Interplanetario, CNR, 00133 Roma, Italy
[5]Demokritos University of Thrace, 67100 Xanthi, Greece
[6]Jet Propulsion Laboratory, California Institute of Technology, Pasadena, CA 91109, USA
[7]Universities Space Research Association, at NASA/Goddard Space Flight Center, Greenbelt, MD 20771, USA
Received 13 October 1997 – Accepted 18 February 1998

Abstract. The International Symposium on Solar-Terrestrial Coupling Processes was held in Paros, Greece, on June 23-27, 1997. The Symposium was sponsored by NASA, the European Geophysical Society, the Greek Ministry of the Aegean, and the Greek Ministry of Development. It was attended by 85 scientists from 13 countries, and included six sessions on topics ranging from Interplanetary Disturbances to Particle Acceleration. In addition to the six sessions a panel discussion session was held. Seven scientists reported on recent advances, open questions and future directions in solar-terrestrial research. This review paper is based on the panelists' reports and includes individual sections on seven particular topics of special interest to solar-terrestrial research. The topics range from the significance of solar wind composition and interplanetary disturbances to promising new technologies and methods. Solar-terrestrial research deserves the special attention of the scientific community, both because of the attractive physics underlying the various phenomena associated with them, as well as because of the applied aspect of the sometimes destructive effects of solar-terrestrial coupling on a wide variety of technological systems.

1 Introduction

This paper is a collaborative review that originated in the panel discussion of the Paros Symposium on Solar-Terrestrial Processes. The contributions to this paper were prepared by the panelists and pursued the following goals:

1. To summarize the current understanding of the chain of processes pertaining to solar-terrestrial coupling.

2. To address important recent findings and outline their importance.

3. To identify open questions and outline their importance/relevance to key issues in solar-terrestrial coupling.

4. To recommend directions for future efforts and developments in our discipline.

The organization of the paper is as follows:

In Section 2 Emmanuel Sarris highlights the importance of superthermal particles in high-β interplanetary and planetary magnetoplasmas, which have long been neglected. He refers to relevant Voyager and Ulysses observations in interplanetary space and in the Jovian magnetosphere.

In Section 3 Johannes Geiss refers to the differences in composition between the two main types of solar wind flow. He suggests that appropriate measurements of element composition and ion charges in the solar wind would yield significant information on solar-terrestrial coupling.

Bruce Tsurutani in Section 4 examines possible interplanetary mechanisms for the creation of the largest magnetic storms in geospace. The examination of profiles of the most intense storms from 1957 to the present indicate that double IMF (Interplanetary Magnetic Field) B_z events are the most probable cause of the largest storms.

Manfred Scholer reports on problems in magnetopause physics in Section 5. His report includes discussions on steady state reconnection, flux transfer events, reconnection under northward IMF, the problem of diffusion and cusp entry.

Wolfgang Baumjohann reports on the much-debated process of magnetospheric substorms in Section 6. He refers to recent findings with the AMPTE/IRM and Geotail spacecraft, and to open questions regarding substorm onset and substorm-associated reconnection in the magnetotail.

In Section 7 Dimitris Vassiliadis reports on Space Weather and its forecasting, and on the new opportunities it will provide in applied and interdisciplinary

Correspondence to: I. A. Daglis

research. He gives a summary of several research directions in current development and some recommendations for the field's evolution.

The terrestrial factor in solar-terrestrial coupling is discussed by Ioannis Daglis in Section 8. He reviews the importance of the terrestrial ionosphere for dynamic processes in geospace, and presents recent advances with regard to the role of ionospheric ions in magnetic storms and substorms.

Last but not least, the high potential of Neutral Atom Imaging (NAI) is outlined by Stefano Orsini in Section 9. He describes the basics of the NAI technique, refers to actual observations, and discusses the focal points for the use of NAI in magnetospheric research.

2 The importance of superthermal particles in high-beta plasmas

In space plasmas the value of the plasma parameter beta (β), i.e. the ratio of the thermal pressure of the plasma to the magnetic pressure, has important consequences in controlling the interaction of the solar wind with the planetary magnetospheres, the shock structure, the properties of the magnetosheath plasma etc. In interplanetary space β is usually in the range 0.1 to 1.0 (Russell, 1990). In computing β the contribution of the superthermal particles to the plasma pressure is assumed negligible. Indeed, numerous observations have established that the energy density of the magnetic field usually exceeds that of the energetic particles (E$\geq$30 keV) by 2 to 3 orders of magnitude. The energetic particles are considered tracers inside the magnetoplasma. The dominant role of the magnetic field in guiding the transportation of energetic particles in interplanetary and magnetospheric plasmas constitutes a basic understanding of the physics of particle propagation.

However, a series of measurements of energetic particles and magnetic field by the Voyager and Ulysses spacecraft have shown that there are certain periods and regions in interplanetary space when the energy density contained in the superthermal tail of the particle distribution is comparable to and occasionally exceeds that of the magnetic field creating conditions of very high-β plasma.

During these periods and/or locales, the hot plasma pressure alone, i.e. the pressure of energetic particles with E$\geq$30 keV not including the thermal plasma pressure, is sufficient to balance the magnetic field pressure ($B^2/2\mu_0$).

The interplanetary events detected by the Ulysses/HI-SCALE experiment (Kasotakis et al., this volume, 1997) when the ratio of the energetic particle pressure to that of the magnetic field exceeds 1, correspond to regions:

a. of unusually large magnetic field depressions

b. in the vicinity of large transient disturbances associated with shock waves.

The presence of these high-β plasmas in the interplanetary space has important implications for:

- The propagation of energetic particles; contrary to the basic understanding of energetic particle propagation, energetic particles cannot be tightly bound to the magnetic field within regions, where their energy density contributes most of the pressure.
- The structure and strength of interplanetary shocks, as well as the properties of the nearby upstream and downstream regions.
- The interaction of the solar wind with the planetary magnetospheres, which is controlled by the total pressure balance and determines the spatial extent and shape of the magnetosphere.

In magnetospheric plasmas the energetic particle pressure is frequently an important or even dominant component of the plasma pressure (e.g., Daglis and Axford, 1996). High-β plasmas are a well known characteristic of the terrestrial ring current (e.g., Daglis et al., 1993; Hamilton et al., 1988; Lui et al., 1987; Williams, 1983), although limited to only a rather small range in radial distance (around $\sim$5 R_E). Most important are the high-β (up to $\sim$200) conditions encountered in many locations throughout the Jovian magnetodisk inside the plasma sheet proper (Krimigis et al., 1981; Lanzerotti et al., 1993), where the energetic particle pressure provides most of the plasma pressure, is comparable to the solar wind pressure and controls the spatial extent and dynamic state of the Jovian magnetosphere .

High-β plasmas within the planetary magnetospheres are often loaded with energetic heavy ionospheric ions of high energy density (Daglis, 1997a; Daglis et al., 1991b, 1994). Heavy ions such as O^+ can play an important role in shaping the magnetosphere and/or contribute to breaking the unstable regime in the magnetotail plasma sheet (e.g., Baker et al., 1982; Büchner and Kuska, 1997; Lakhina, 1995; Swift, 1992).

3 Variations in solar wind composition: Clues on magnetospheric entry and transport

There are two main types of solar wind flow, the slow wind coming from the streamer belt, and the fast streams coming out of the coronal holes. During solar minimum conditions, these holes are centered around the poles of the Sun. However, because their shapes are irregular and the outflow from them is superradial (i.e., the flow lines diverge stronger than radial), the fast streams can reach the low latitude region of the heliosphere. Especially during declining solar activity and under solar minimum conditions, the Earth is repeatedly moving into and out of a fast stream, due to the solar rotation (Bame et al., 1977).

Elemental and isotopic abundances in the solar wind are not exactly the same as they are in its source reservoir, the outer convective zone (OCZ) of the Sun. Sepa-

ration processes in the chromosphere and in the corona produce a general variability in solar wind ion abundance as well as systematic differences between solar wind and OCZ composition. The most systematic difference is produced in the chromosphere. There, an ion-atom separation process causes an overabundance of elements with low first ionization potential (the "FIP-effect") and an underabundance of helium in the plasma that is fed into the corona. The FIP effect is strong in the slow wind, but it is weak in the fast streams (Gloeckler et al., 1989; von Steiger et al., 1992).

Solar wind and solar flare particle abundance data (Garrard and Stone, 1994; von Steiger et al., in press, 1997), covering a dozen elements, indicate that the FIP effect results from a competition between ionization time in the outer chromosphere and a characteristic ion-atom separation time. However, specifics concerning the dynamics and geometry of separation remain to be specified (Henoux and Somov, 1992; von Steiger et al., in press, 1997). It is well known that ion-atom separation also plays an important role in the environment of the Earth, for instance in forming the E-layers or in the fractionation of the ions that are moving into the plasmasphere (Geiss and Young, 1981). Comparison of concepts of ion-atom separation in the Earth's environment and in the Sun's chromosphere could be beneficial to both research fields.

The boundaries of coronal holes are very sharp (Huber et al., 1974), and thus, also the boundaries between the slow solar wind and the fast streams are well defined. Three main solar wind parameters change at these boundaries. The speed in the fast streams is higher by nearly a factor of two, the average charge states of heavier elements are lower as the result of the lower electron temperature in the coronal holes, and the abundances of elements like Mg, Si and Fe are lower, due to the reduced strength of the FIP effect (Fig. 1). Studies with SWICS/Ulysses have shown that these changes occur regularly and simultaneously, with time delays of less than a day (Geiss et al., 1995; Wimmer et al., in press, 1997).

The systematic difference in the ion charge states and the chemical composition between the slow wind and the fast streams offers an opportunity to study magnetospheric entry of solar wind ions into the magnetosphere and loss processes from the magnetosphere. Aside from density enhancements in shocks which are associated with the interaction between the two solar wind regimes (A. J. Lazarus, personal communication, 1997), the average momentum flow is not very different in the slow wind and in the fast streams. Thus, we have large changes in the composition of minor constituents without a major difference in the solar wind pressure. These are favorable conditions for tracer studies. Suitable pairs of ions can be used to monitor solar wind entry, transport inside the magnetosphere, residence times, loss rates and ion recombination processes.

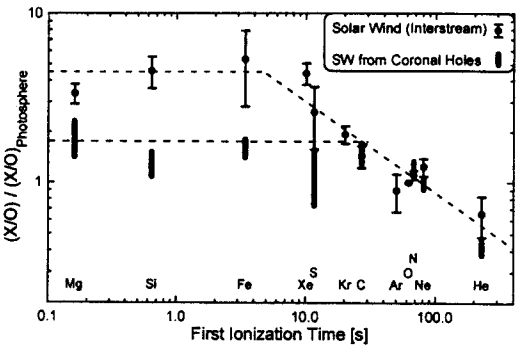

Fig. 1. Solar wind abundances, relative to photospheric abundances and normalized to the oxygen, as a function of the first ionization time (after von Steiger, 1995). This is the ionization time of atoms for an optically thin layer at the solar surface. The FIP effect, i.e. the overabundance of elements with low first ionization potential, is strong in the slow solar wind (or interstream wind) and relatively weak in the fast streams coming out of coronal holes.

Ideal instruments for such studies would be time-of-flight mass spectrometers which determine ion masses as well as mass/charge ratios (Gloeckler, 1990). Suitable as tracers would be the charge states of carbon, oxygen, and iron, as well as abundance ratios between low- and high-FIP elements. Here are a few examples: Fe^{16+} is common in the slow wind, but virtually absent in the fast streams, resulting in a difference of the $Fe^{16+}/Fe^{8+\ to\ 11+}$ ratio by more than a factor of 10 between the two types of solar wind. The highest charge state of Mg in the solar wind is Mg^{10+} and the lowest charge state of O is O^{6+}. Thus the differences in element composition and ion charges combine to give a change in the Mg^{10+}/O^{6+} ratio by a factor of five to seven between the slow wind and fast streams. The changes in ion abundance ratios given in these two examples are so large that the method advocated here could give significant information on magnetospheric processes, even with limited counting statistics.

4 Interplanetary causes of great and super - intense magnetic storms

4.1 Introduction

The purpose of this section is to examine the causes of great (Dst < −250 nT) magnetic storms at the Earth. We consider the effects of interplanetary shock events on magnetic cloud and sheath plasma, leading to potentially stronger interplanetary magnetic field (IMF) magnitudes. We also examine the effects of a long-duration southward sheath magnetic field, followed by a magnetic cloud B_s (southward IMF) event. The profiles of

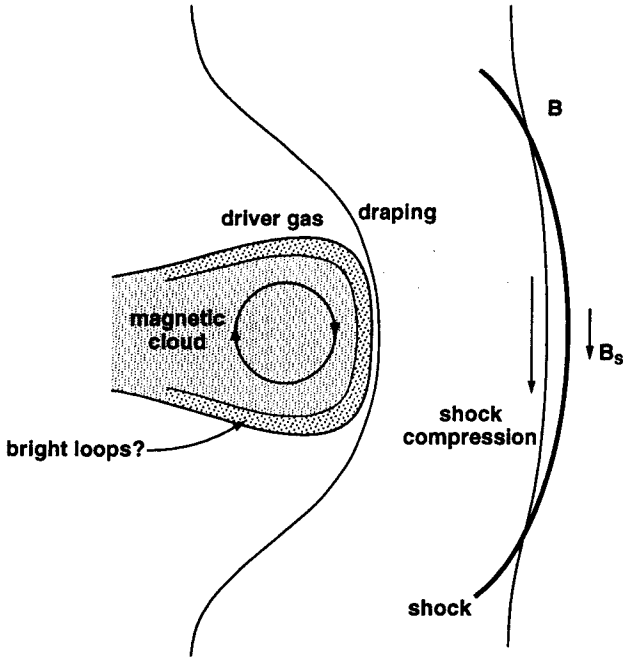

Fig. 2. Schematic showing geometry of a magnetic cloud and upstream sheath.

the most intense storms for which interplanetary data exist are discussed in light of these mechanisms.

We know the energy transfer mechanism from the solar wind to the magnetosphere for magnetic storms is magnetic reconnection between the interplanetary magnetic fields and the Earth's fields (Dungey, 1961), where the interplanetary dawn-dusk electric field is given by – $V_{sw} \times B_s$. In the above expression, V_{SW} is the solar wind velocity and BS is the southward component of the interplanetary magnetic field (IMF). However, there has been little effort placed to date on understanding the detailed causes of the very largest magnetic storms. Are the velocities unusually high? Are the magnetic fields unusually intense or do both the velocity and magnetic fields have to be large to create superintense storms? Are double (or triple) shock events creating very high magnetic fields? Or are there other causes of these unusually intense storm events?

4.2 Sheath/ICME magnetic fields

It has been shown that a southward IMF $\leq$ –10 nT ($E_{sw} \geq 5$ mV/m) for T>3 hours is necessary for the creation of an intense ($Dst \leq$ –100 nT) magnetic storm (Gonzalez and Tsurutani, 1987). The southward IMF events can be located either in the sheath fields ahead of fast interplanetary coronal mass ejections (ICMEs) or within the ICMEs themselves. The latter case, B_S within an ICME, is usually in the form of a magnetic cloud (Burlaga et al., 1981). A schematic of this overall geometry is given in Fig. 2. However it should be

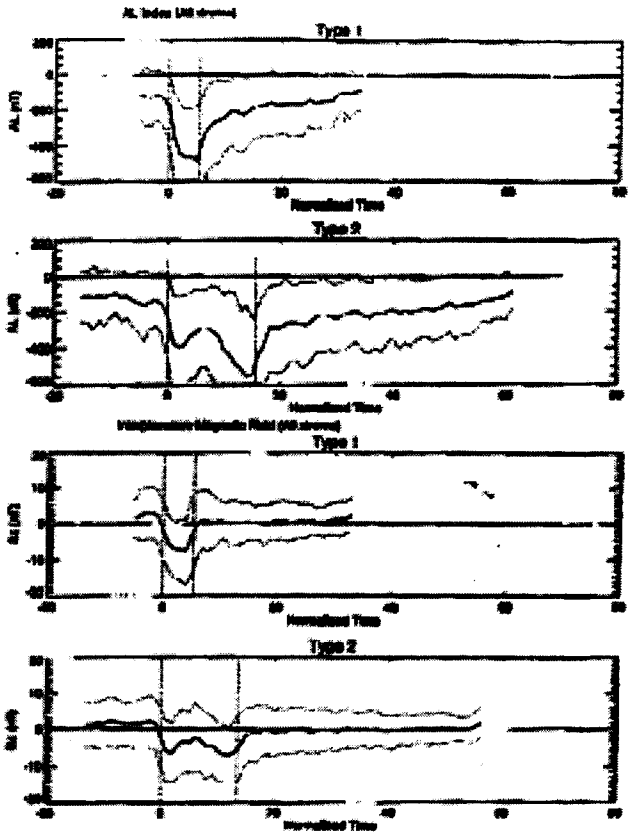

Fig. 3. Normalized time series of: (a) the AL index showing the development of single and double geomagnetic storms (upper two panels), and (b) the corresponding IMF B_z components (lower two panels) showing the southward turning of the field which induces the response in the AL index shown in (a) (from Kamide et al., 1997b).

pointed out that 5 out of 6 fast solar ejecta do not contain magnetic clouds (Tsurutani et al., 1988a).

There are reasons to expect stronger magnetic fields in both the fast ICMEs and the upstream sheaths. A fast driver gas will in general lead to stronger shock-compressed magnetic fields (depending on the upstream flow conditions). The magnetic field compression across the shock can be up to a maximum of 4 (Kennel et al., 1985). If the upstream IMF has a southward orientation, the shock leads to intensification of this component.

In previous data analysis results, there has been a general relationship between the speed of the ICME and the magnetic field intensity in the magnetic cloud. From the Burlaga et al. (1978) data set, we note that the magnetic field intensity of slow speed streams was only ~10 nT, whereas the faster clouds have intensities of 20-30 nT. This relationship has not been previously pointed out and no theoretical explanation has been offered. Compression of the cloud is certainly occurring, but it is uncertain whether all of the field increase can be accounted for by such an effect. Another possibility is that this relationship may be related to the CME release and acceleration mechanisms at the Sun. The |B|-V_{sw} relationship may give important clues as to these mechanisms. This topic is examined in greater detail in Tsurutani et al. (this volume, 1998).

One mechanism to create field strengths even higher than that addressed above, would be for a second interplanetary shock to (further) compress the high fields existing in the ICME/sheath regions (of Fig. 2). An argument was presented in Tsurutani and Gonzalez (1997) that the presence of shocks/strong compressions may not be possible within magnetic clouds, because of the low β in these regions. Typical β values in clouds are ~0.1 with consequential Alfvén/magnetosonic speeds of 300–700 km/s. These high speeds necessary for shock formation, should ordinarily preclude the formation of such structures within magnetic clouds.

It is unclear what will happen to this compressional wave when it reaches the antisolar side of the cloud. It may be sufficiently dispersed or it may possibly reform as a shock. Another mechanism to have shocks occurring within sheaths is to have the shocks propagate from the downstream magnetosheath up into the front side sheath regions. To determine what the possibility of each of these mechanisms might be, simulation efforts are recommended.

4.3 Double storms

Another way to get large *Dst* events is to have two storm main phases with the second closely following the first. Kamide et al. (1997b) in an analysis of more than 1200 magnetic storms has shown that such events are quite common and are caused by two IMF southward field events of approximately equal strength (Fig. 3). Kamide et al. (1997b) argue that this could also be

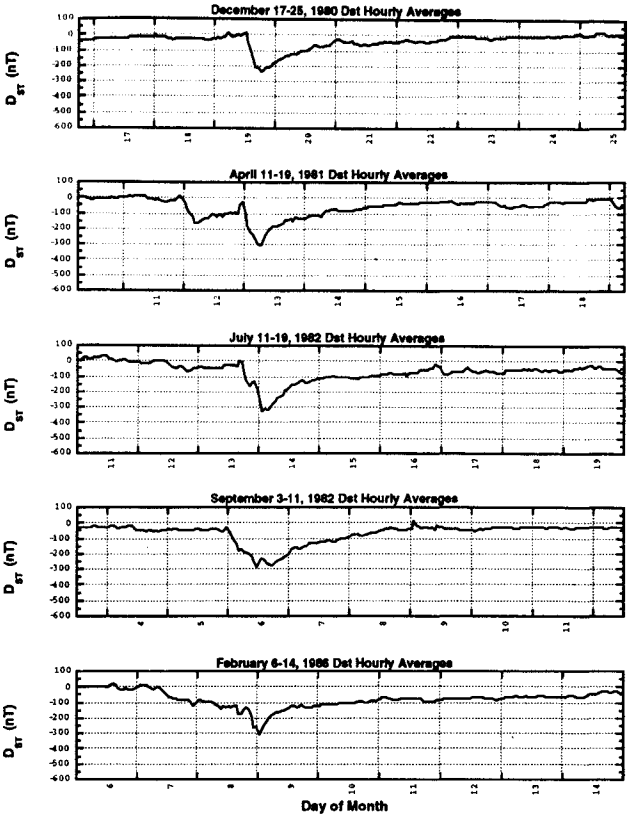

Fig. 4. The five largest magnetic storms during the period from 1980 through 1986.

viewed as two moderate magnetic storms with the *Dst* base of the second well below that of the first.

Grande et al. (1996) and Daglis (1997a) have studied the March 23, 1991, double magnetic storm using CRRES ion composition data. Grande et al. point out that the first event is dominated by Fe^{9+}, whereas the second by Fe^{16+}. A likely explanation is the first event was caused by sheath southward IMFs (shocked, slow solar wind plasma and fields) and the second was from the remnants of the ICME itself (magnetic cloud). The peak *Dst* for the first event was ~–100 nT and ~–300 nT for the second event. We note however that these values were not solar wind ram pressure-corrected. The field at the storm initial phase was ~+60 nT indicating that the correction will be substantial.

We reexamine the interplanetary causes of great magnetic storms ($Dst \leq$ –250 nT) which have corresponding interplanetary data (reported in Tsurutani et al. (1992)). The *Dst* profiles are shown in Fig. 4. Three of the four largest events have complex main phases. The April 12-13, 1981 and July 13-14, 1982 events are double main phase storms. The February 7-9, 1986 storm had a main phase that took 1 1/2 days to develop, then an abrupt further decrease. This could be due to a complex ICME sheath region.

4.4 Conclusions

It is found that double main phase events are quite common for great magnetic storms (Dst < -250 nT). The two (or more) ring current injections lead to the exceptionally large Dst values as suggested by Kamide et al. (1997b). A reexamination of the IMF B_S features leading these five storm events would be illuminating.

5 Problems in magnetopause physics

5.1 Introduction

The magnetopause is the outer boundary of Earth's magnetosphere. There is abundant evidence that the magnetopause is the site where solar wind mass, energy, and momentum is constantly being transferred to the magnetosphere. A wide variety of processes has been proposed in order to accomplish this transfer. Steady-state processes include diffusion, magnetic reconnection, and direct cusp entry. Transient processes include bursty reconnection, impulsive penetration, and non-linear Kelvin-Helmholtz instability. We will briefly describe the characteristics of some of these mechanisms, comment on the significance to plasma transfer in and out of the magnetosphere, and point out open questions.

5.2 Steady state reconnection

The magnetopause is most easily described as a current sheet that separates two plasma regions with different magnetic fields. When anti-parallel magnetic field components exist on the two sides any deviation from the ideal MHD behavior of the plasma allows magnetic field lines embedded in the magnetosheath to connect with the magnetospheric field lines, as first proposed by Dungey (1961). Solar wind plasma can then flow along the reconnected field lines into the magnetosphere, thereby adding mass, energy and momentum to the magnetospheric plasma population. Furthermore, the newly reconnected field lines are highly bent and the magnetic tension force accelerates the plasma to high speed. Much of the in-situ evidence for reconnection at the magnetopause comes from the observations of the accelerated flows (Sonnerup et al., 1995). Evidence for reconnection has also been found from features in the plasma distribution function (Cowley, 1982) and from spatial profiles of ions compared to electrons exhibiting a velocity filter effect (Gosling et al., 1990). While it is clear that reconnection occurs, it is less clear why this is so. In one-fluid MHD, reconnection is governed by the diffusion term in the generalized induction equation. Near the neutral line a finite resistivity η allows an electric field along the neutral line in the so-called diffusion region. The diffusion term is based on Ohm's law, which describes the relation between the electric field and the current. In the simplest case the electric field in the moving frame and the current are proportional to each other, the proportionality factor being the resistivity. In the case of a collisionless plasma such a resistivity may be provided by an instability, e.g., by a current driven instability. In case if such an anomalous resistivity is not present other processes have to supply an electric field along the neutral line. Assuming quasi-neutrality, the electric field can be determined by the electron momentum equation

$$\mathbf{E} = -\frac{4\pi}{\omega_{pe}^2}\frac{d\mathbf{j}}{dt} - \frac{1}{nec}\mathbf{j}\times\mathbf{B} + \frac{1}{c}\mathbf{v_i}\times\mathbf{B} - \frac{1}{e^2 n}\nabla\cdot\underline{\mathbf{P_e}} + -\eta\mathbf{j}$$

Here $\underline{\mathbf{P_e}}$ is the full electron pressure tensor, ω_{pe} is the electron plasma frequency, $\mathbf{j}$ is the electrical current, $\mathbf{v_i}$ the bulk velocity of the fluid (ions), and n is the number density of both ions and electrons. Magnetic flux is unfrozen in the ion frame when $\nabla\times(\mathbf{E}+\mathbf{v_i}\times\mathbf{B}/c) \neq 0$. This can be achieved by, besides finite resistivity, either of the following three: an electron pressure tensor $\underline{\mathbf{P_e}}$ with non-zero off-diagonal terms, the term $(4\pi/\omega_{pe}^2)d\mathbf{j}/dt$ due to electron inertia, or an electron equation of state where the pressure is not barotropic but baroclinic, i.e., isobars and isodensity surfaces do not coincide (Scudder, 1997). It is evident that the details of the electron behavior are of fundamental importance in understanding magnetic reconnection in collisionless plasmas in general and at the magnetopause in particular. Observationally this requires high spatial and temporal resolution of the electron distribution function: the typical electron scale, the electron skin depth c/ω_{pe}, is at the magnetopause of the order of 1 km.

5.3 Flux transfer events

Short-lived abnormal deflections in the magnetic field near the magnetopause are called "flux transfer events", or FTEs for short. Such signatures may occur on the magnetosheath side as well as on the magnetospheric side of the magnetopause, and are called magnetosheath events or magnetospheric events. Most models of FTEs rely in some way on time dependent magnetic reconnection between the IMF and the Earth's magnetic field. They differ by how often a magnetic field line is reconnected, by the length of the reconnection line(s) and by the process initializing reconnection (Scholer, 1995). In the multiple neutral line model the tearing mode produces magnetic islands, which grow (due to the continuous injection of the solar wind toward the magnetopause) to considerable size (Lee and Fu, 1985). In the presence of a shear magnetic field component the islands become flux tubes embedded in the magnetopause. A second model is based on a combination between the Kelvin-Helmholtz instability and the tearing mode instability at higher latitudes on the dayside when a strong velocity shear exists across the magnetopause current layer (Pu et al., 1990). The large-scale vortices resulting from the Kelvin-Helmholtz instability twist the mag-

netic field; reconnection sets in above and below the fluid vortices leading to flux ropes in the presence of a B_y component. In these models it is not clear how the connectivity occurs at the ends of the flux ropes. In the single X-line reconnection model sudden onset of reconnection leads to a pair of bulges in the magnetopause extending over a large longitudinal segment (Scholer, 1988). As far as magnetic connectivity is concerned this model is a truly two-dimensional model. The original elbow-shaped flux transfer model by Russell and Elphic (1978) describes the FTE as a magnetosheath flux tube connected to the magnetospheric magnetic field through a slanted hole in the magnetopause. Three-dimensional MHD simulations have led to two global models. Repeated reconnection at higher latitudes of the dayside magnetopause under strictly southward IMF can lead to flux tubes with a twisted field line structure extending in the dawn-dusk direction (Sato et al., 1986). Inclusion of a B_y IMF component in global simulations has produced flux tubes extending from high latitudes at the dawn side of one hemisphere to high latitudes on the dusk side of the opposite hemisphere (Ogino et al., 1989). Another model is based on both patchy and intermittent reconnection: the reconnection sites at higher latitudes are determined by three-dimensional tearing (X-lines do occur only along short segments) and the reconnection rate at each reconnection site is determined by the component reconnection driven by the solar wind (Kan, 1988).

A way to differentiate between the various FTE models is to determine the magnetic connectivity. Magnetic connectivity is very simple in the bursty single X line model and the elbow-shaped flux tube model whereas it is more complicated in the multiple X line reconnection model and is unclear in some of the other models. From the theoretical point of view the problem of connectivity has to be pursued further. Observationally, anisotropy measurements of energetic magnetospheric particles should be able to give some indication of the connectivity. There are also differences in the amount of twist of the connected flux tubes predicted for some of the models. Twist is difficult to measure; however, measurements with several not too widely separated spacecraft can give some answer.

Another difference between some models is the orientation of the flux tube and, partly connected with this, the length of the neutral line. It is unclear whether the magnetopause is unstable to the drift-tearing mode instability. If the number of growing modes is sufficiently large, the nearby magnetic islands overlap and magnetic field lines wander stochastically between them. This leads to diffusion of magnetic field from one side of the layer to the other. Such a percolation process has so far not been verified directly by spacecraft observations. Also the importance of percolation for flux transfer events has yet to be demonstrated. The interpretation of many IMF perturbations near the magnetopause in terms of FTEs has been criticized by Sibeck (1992): some of the perturbations may well be explained in terms of the passage of pressure-pulse-induced magnetopause ripplets across an observing satellite.

5.4 Reconnection under northward IMF

Steady state reconnection and bursty reconnection are expected under southward IMF and will leads to a low-latitude boundary layer (LLBL) on open field lines. There is indeed abundant evidence that the LLBL is at times on open field lines, i.e., magnetospheric field lines having one foot in the ionosphere and extending into the magnetosheath. There is more circumstantial evidence that the LLBL also exists on closed field lines over some portion of the magnetospheric boundary. Nishida (1989) has proposed that when the interplanetary magnetic field (IMF) is northward transient and localized reconnection may occur on the dayside magnetopause and may lead to the formation of the LLBL. In this model the momentum in the solar wind in the magnetosheath is transported into the LLBL directly with the entering plasma and indirectly as the reconnected field lines are pulled by the solar wind plasma. Only those geomagnetic field lines will contain magnetosheath plasma that have been open at some time in the past. Thus, according to this model, the LLBL is an entity of flux tubes which have well-defined boundaries. The blobs observed by Sckopke et al. (1981) are taken as evidence for such well-defined flux tubes.

Magnetic reconnection at high latitudes behind the polar cusps has been proposed by Song and Russell (1992) as a process for the formation of the LLBL under northward IMF: a magnetosheath flux tube, which drapes over the stagnation point, moves relatively slowly with respect to the magnetospheric fields and is likely to reconnect at high latitudes, where the magnetosheath and the lobe field are antiparallel. After reconnection the poleward portion of the flux tube convects tailward with the solar wind flow. In the dayside portion of the flux tube the magnetospheric and the magnetosheath plasmas mix and the flux tube sinks into the magnetosphere. During this process the flux tube length shortens and the diameter decreases, assuming that the flux tube field is the same as the magnetospheric field when it enters the magnetosphere.

Fuselier et al. (1995) have presented evidence that reconnection does not necessarily occur simultaneously as proposed in the qualitative Song and Russell (1992) picture. They identified a magnetosheath boundary layer (MSBL) near the dayside magnetopause at the magnetosheath side of the magnetopause current layer and the LLBL. This MSBL is characterized by unidirectional streaming electrons: one half of the distribution parallel to the magnetic field has the characteristics of the distribution in the nearby magnetosheath (actually in the plasma depletion layer), the other half is similar to the

distribution in the LLBL on the Earthward side of the current layer. The existence of such an MSBL suggests that reconnection does not occur simultaneously at both high latitude reconnection sites.

The process of high latitude reconnection and magnetospheric incorporation of newly closed flux tubes is a persistent feature of global magnetospheric simulations. For example Raeder et al. (1995) found that the reconnection-produced newly closed field lines at the dayside are swept by the magnetosheath flow along the magnetopause and are stretched along the flanks of the tail. The momentum flux of the magnetosheath is supposedly so large that the field lines become stretched to at least 400 R_E downtail. These stretched field lines constitute a tailward-flowing layer with closed field lines, i.e., with positive B_z, while there may still exist negative B_z near the tail axis from earlier or still ongoing near-Earth reconnection. This tail flank boundary layer (TFBL) does not seem to be driven by a process similar to the one proposed by Song and Russell (1992) where thermal energy is converted into dynamic energy; rather, the momentum of the magnetosheath flow in a newly produced closed flux tube propels the flux tube downstream. Solar wind flow energy is converted by this process into electromagnetic energy by the stretching and twisting of the flux tubes. It is still unclear which part of the LLBL is on closed/open field lines and under which conditions and whether or not the flanks are more important for the formation of the magnetopause boundary layer and in the coupling than the dayside LLBL. Clarification of these problems will require a substantial amount of additional experimental and theoretical work as well as all types of numerical simulations.

5.5 The problem of diffusion

Because of the mutual topologies of the draped IMF and the warped magnetospheric field, there is probably always reconnection somewhere at the magnetopause, leading to free plasma entry. Only when the sheath field is purely northward may diffusion be assumed to explain the filling of the LLBL at the flanks. The experimental investigation of the anomalous diffusion process has not given support to theories based on diffusive particle transport from the solar wind to the LLBL. Precise analyses of wave observations by Tsurutani et al. (1989) and Treumann et al. (1991) showed that the wave intensities in the transition layer are not strong enough to yield the required anomalous collision frequencies. The canonical value of the diffusion coefficient required for the filling of the LLBL is about $D \approx 10^9$ m^2s^{-1} (Sonnerup, 1980). The most promising instability is the lower hybrid drift instability (LHDI), which results in the highest diffusion coefficient at a given wave electric field intensity. The highest measured wave intensities result in a diffusion coefficient, which comes close to the Sonnerup diffusion limit. Thus sporadic, very high intensities in this mode may cause strong plasma injection. However, a statistical analysis of the wave intensities by Treumann and Bauer (1996) obtained from a large sample of magnetopause crossings shows that the average intensity is below 10^{-7} V^2m^{-2} which yield extremely small average diffusion. Thus diffusion can only be marginally high in microscopic localized regions, presumably LH density cavitons which escape the measurements. High temporal and spatial resolution wave measurements are required to obtain new insight. Anomalous diffusion based on low frequency magnetic fluctuations has been ruled out (Tsurutani and Thorne, 1982). However, if the low frequency waves measured by Rezeau et al. (1993) are kinetic Alfvén waves, in particular Alfvén solitons, then they are another candidate leading to particle diffusion in a large resonant phase space volume. For these low frequencies the first adiabatic invariant is conserved, diffusion can therefore only be caused by scale invariant turbulence (Scholer and Treumann, 1997).

Although electric wave intensities at the magnetopause are unlikely to lead to anomalous diffusion, the resulting anomalous collision frequency is high enough for locally providing an anomalous resistivity required by reconnection. The highest electric wave intensities result, assuming an electron temperature of 50 eV and a magnetic field of 100 nT, in a collision frequency of 10 - 50 Hz, which is more than 6 orders of magnitude higher than the collision frequency based on Coulomb collisions. Thus reconnection based on anomalous resistivity near the magnetopause cannot be ruled out, what brings us back to the question what causes collisionless reconnection at the magnetopause.

5.6 Cusp entry

The cusp region is the most unexplored from the observational as well as from the theoretical point of view. Due to the convergence of the magnetospheric magnetic field toward a point in the cusp there will always be a point where the IMF is antiparallel to the magnetospheric field. This region can be a preferential region for reconnection which may lead to direct entry of solar wind plasma into the magnetosphere. The bulges of flux ropes representing flux transfer events move on the dayside to higher latitudes and eventually encounter the cusps. It has been proposed that the FTE plasma bubble will break up once the speed of the bubble becomes smaller than the Alfvén speed in the medium ahead of the bubble (Smith and Lockwood, 1990). Ion precipitation signatures on cusp field lines have been predicted on the basis of the pulsating cusp model, i.e., assuming the occurrence of time-varying magnetic reconnection at the dayside magnetopause. During steady-state reconnection the cusp is expected to be a rotational discontinuity, whereas during pulsed reconnection the cusp may alternate between a RD and a tangential discontinuity.

The magnetosheath flow over the funnel-shaped in-

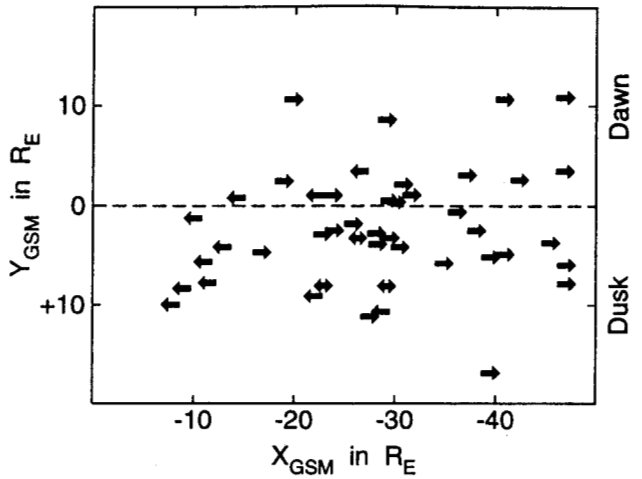

Fig. 5. Location of 27 fast tailward convection flows, 11 fast Earthward convection flows, and 3 reversal events (first Earthward and then tailward) observed by Geotail. All events had velocities perpendicular to the magnetic field in excess of 300 km/s (after Nagai and Machida, in press, 1997).

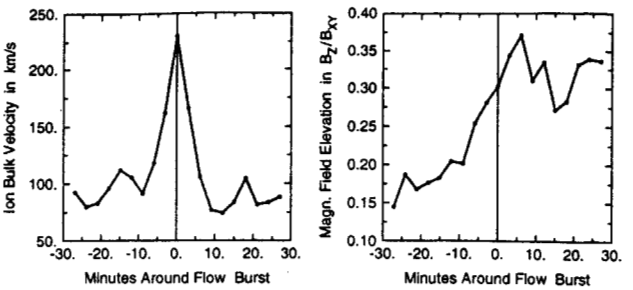

Fig. 6. Results on a superposed epoch analysis applied on plasma and magnetic field data around more than 100 bursty bulk flow events observed by IRM in the inner central plasma sheet during 1995. The data are centered around the flow burst maximum and averaged in 3-min bins (after Baumjohann, 1993).

dentation of the magnetopause in the cusp is expected to lead to turbulence. The turbulence may lead to eddy diffusion which can populate the cusp boundary layer with magnetosheath plasma (Haerendel, 1978). From the coherence time of 20 sec measured by the Heos-2 spacecraft a diffusion coefficient of 5×10^{10} m^2/sec was derived. This exceeds the Bohm diffusion limit and corresponds to free streaming. If this applies, the cusp region is a region of free plasma inflow. The turbulent flow expected in the cusp should also lead to turbulent reconnection.

6 Substorms

6.1 Recent findings and current understanding

During the last decade the near-Earth neutral line (NENL) model has been challenged for a number of reasons (e.g., Baker et al., 1996). The most important one was that AMPTE/IRM and ISEE 1/2 did observe high-speed Earthward flows, but rarely fast tailward flows within their apogees (Angelopoulos et al., 1994; Baumjohann, 1993). Hence, the NENL is typically not situated at 15-20 R_E radial distance, as originally assumed.

However, recent results from Geotail, summarized by Nagai and Machida (in press, 1997) and redrawn in Fig. 5, show a transition from Earthward to tailward convective flows, i.e., flows perpendicular to the magnetic field, at tailward distances of 22-30 R_E, just outside of the ISEE orbit. Furthermore, the flows near this site are found to precede the ground onset time in a number of cases, implying that magnetic reconnection at a NENL is indeed the cause of substorms.

Another argument against the NENL model was the apparent mismatch between the brightening of the equatormost auroral arc, which typically maps to 10 R_E or less and therefore not to the 22-30 R_E tailward distance of the NENL. However, as Haerendel (1992) already pointed out five years ago, there is no need for these two locations to map to each other. In fact, both locations are connected by the bursty fast flows shown in Fig. 6.

It is the high-speed flow, which causes the first near-Earth signatures of substorm onset. Shiokawa et al. (in press, 1998) found that the Earthward high-speed flows are not gradually decreasing in speed, but are braked rather abruptly around 10-15 R_E. The associated flow shear creates a weak current wedge of $\sim 10^5$ A and dipolarizes the magnetic field.

Shiokawa et al. (in press, 1998) did a case study and could show that the sequence of events is ordered as shown in Fig. 7. A high-speed ion flow, supposedly created by an NENL at 20-30 R_E, is braked at the boundary between tail-like and dipolar fields, leading to a dawnward 'inertia' current and magnetic field dipolarization and pile-up. Some minutes later, typical substorm effects like a negative H-component at high and positive H- and D-components at mid-latitudes, indicating the growth of the substorm current wedge, and dispersionless injection of energetic particles at synchronous orbit, are seen further in.

6.2 Open questions and outstanding problems

However, there are two problems with the scenario of Shiokawa et al. (in press, 1998). First, bursty fast flows are seen also during times where no expansion phase signatures are seen on the ground. Secondly, the effects associated with the braking last only as the flow itself, about five minutes, and the current strength is comparatively weak. Actually, it seems likely that high-speed flow braking often causes only a pseudo-onset or a weak short-lived expansion phase, which may remain undetected on the ground because of its localized nature.

Hence, the question 'What causes substorm onset?'

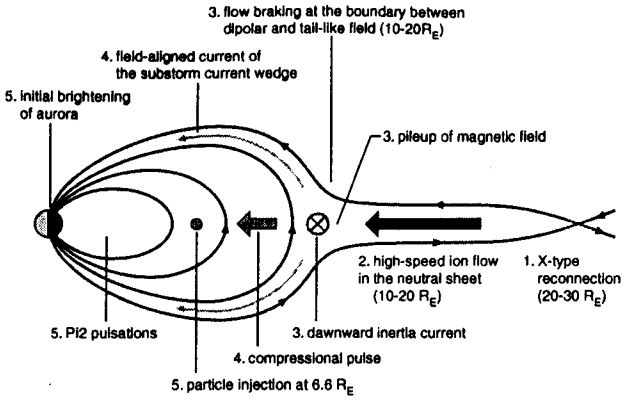

Fig. 7. Model of current wedge formation during the initial stage of substorm expansion. The number preceding each comment indicates the order of occurrence (after Shiokawa et al., in press, 1998).

now seems to boil down to the question what causes an initial brightening or a pseudo-breakup or -onset to develop into a full-fledged substorm. At present the most likely candidate is a kind of feedback with the ionosphere via creation of Cowling channel (J. R. Kan, personal communication, 1997). However, also other processes inside 10 R_E may be needed in order to lead to full substorm growth (Lui et al., 1988).

Another open issue pertains to the question whether open or closed flux is reconnected at the NENL. In the original NENL model, reconnection of open lobe magnetic field and the associated release of the energy stored in that field is an essential ingredient (Baker et al., 1996).

Caan et al. (1973) previously noted that some substorms display depletion of lobe flux and thus near-Earth reconnection of open flux, while more localized substorms and those with multiple onsets do not. Caan et al. (1975) did a superposed epoch study of 20 clear lobe field depletion events and found that all of them were associated with substorms. However, the latter were all clearly isolated substorms associated with a northward turning of the IMF. Since people like to study clear isolated events, the earlier caveat became forgotten and the decrease of lobe field energy density was thought to be associated with all substorms until 1996.

In that year, Nishida et al. (1996) noted that mainly closed field lines are reconnected at the near-Earth neutral line. Independently, Baumjohann et al. (1996) discovered that only those substorm that took place during a storm main phase exhibited a strong decrease in lobe field density, while those occurring during times of low $|Dst|$ did on average not exhibit any significant changes in lobe field strength (see Fig. 8).

Hence, there is a whole spectrum of substorms. Substorms come in all sizes, from pseudo-onsets over weak and/or localized substorms to truly global ones. Different types of substorms may well involve different instabilities, in addition or instead, and only studying the whole spectrum will bring us closer to the final answer. Studying only one type of substorms and developing a model for this type of substorm may be a useful first step, but one should abstain from a one-size-fits-all attitude.

Furthermore, substorms show signatures everywhere in the nightside magnetosphere, from the ionosphere out to 100 R_E, and a real substorm model has to explain all of these features. Analyzing substorms features in a particular region of the tail is useful as a first step, but developing a model that only explains the phenomena seen in that region ranges from useless to even dangerous, if the model is not put into a more global perspective.

At the present time, the oldest substorm model, namely the NENL model, still presents the best basis for a truly global substorm model. However, it should not be taken as a paradigm, but modified and extended to include fast flow braking and feedback from the ionosphere and perhaps inner magnetosphere. Only in that case it will be able to explain the whole range of substorms observed.

7 Geospace activity forecasting

7.1 Introduction

In recent years space physics has been acquiring the foundations necessary for a predictive science. The success of scientific programs such as ISTP (e.g., Mish et al., 1995) is evidence for our ability to relate observations from many parts of geospace. We are now studying how the geospace responds as a system, and we start fitting in this framework the processes that have been studied one at a time for several decades.

Such progress is important for prediction and forecasting capability. Prediction refers to individual events (and, in its more general form, of new physical concepts); we use the term independently of whether the event has actually taken place already (e.g. validation of a model is a study of what its predictions for past events); while forecasting is reserved for prognoses of future events. The high-density, high-quality data that are now becoming regularly available serve to validate and improve the geospace models. Recently, then, the space physics community has started discussing how to apply the geospace models to the systematic monitoring and forecasting of geospace conditions or, as is commonly known, "space weather" (NSWC, 1995, 1997; Siscoe and Maynard, 1996).

Space weather "refers to the conditions on the Sun and in the solar wind, magnetosphere, ionosphere, and thermosphere that can influence the performance and reliability of space-borne and ground-based technological systems and can endanger human life or health. Adverse conditions in the space environment can cause

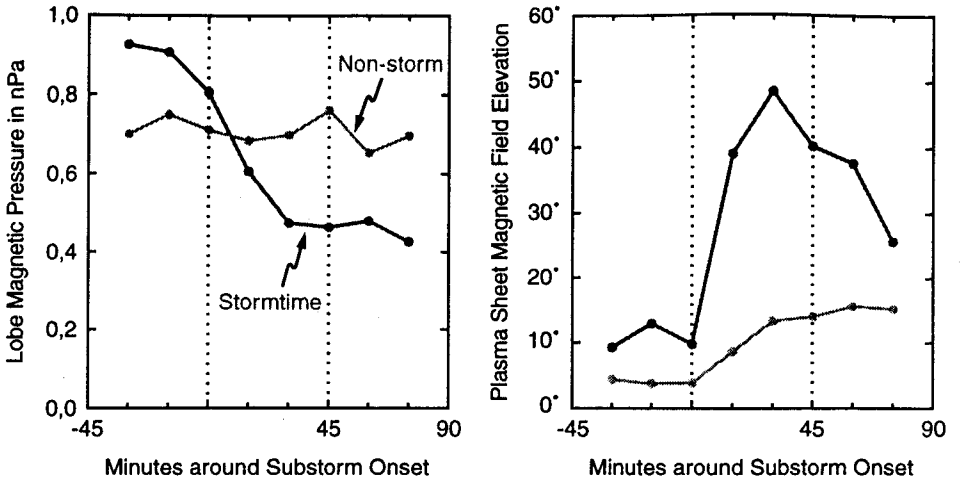

Fig. 8. Superposed traces of the magnetic pressure in the tail lobe (left) and the magnetic field elevation angle in the central plasma sheet (right) during storm-time and non-storm substorms. The traces are constructed by averaging the measured values in 15-min bins with respect to substorm onset, separately for 7 substorms that occurred during the expansion phase of a magnetic storm and 35 substorms where the *Dst* index was above −25 nT. The dashed vertical lines mark substorm onset and the approximate start of the recovery phase (after Baumjohann et al., 1996).

disruption of satellite operations, communications, navigation, and electric power distribution grids, leading to a variety of socioeconomic losses" (NSWC, 1995). It is becoming increasingly evident how disparate the cost of space weather disturbances is, compared to the budgets allocated for studying them. The cost of a telecommunication satellite or of an electric power utility transformer exceeds $100 M. At the same time the vulnerability of the various technological systems affected by space weather, may increase as a result of changes towards less-shielded components, less robust infrastructure, operation conditions, or higher demand and use. In two independent developments, the deregulation of the U.S. electric power utility industry, and the introduction of a new generation of lightweight mobile communication satellites, many of which will be placed in low-Earth orbit, are expected to expand the markets for space weather products.

7.2 Present status

Currently there are modeling, monitoring, and forecasting capabilities for many of the most important geospace disturbances. Among the existing physical models, most important for space weather forecasting are those models whose inputs are conditions on the solar surface or in the solar wind, as these are monitored from ground stations and spacecraft such as WIND, SOHO, and ACE (e.g., Mish et al., 1995; Poland, 1997). These solar wind and interplanetary magnetic field (IMF) conditions are the inputs of models, such as the potential field-source surface models which can propagate the inputs from above the solar surface to 1 AU and can make very good predictions for the velocity, and good predictions for the low-frequency variations of IMF B_z polarity (Hoeksema and Zhao, 1992). Global MHD models are now coupled to solar wind and can reproduce several characteristics of large-scale magnetospheric and high-latitude ionospheric activity (Papadopoulos et al., this volume, 1997). Inner-magnetosphere test-particle models can reproduce particle fluxes and electric fields observed during individual storms in impressive detail, while the Magnetospheric Specification and Forecast Model (Freeman et al., 1994), based on solar wind input and geomagnetic activity index estimates, can now reproduce changes in electron fluxes due to spatial or temporal effects with an accuracy of less than one order of magnitude. Closer to Earth, ionospheric models demonstrate the effects of ionospheric disturbances, while electrodynamic models can represent the effects of space weather on geomagnetically induced currents (Viljanen and Pirjola, 1995).

Even faster and more accurate than the physical models at this stage are the empirical models. The starting point for these models are solar wind, magnetosphere and ionosphere key parameters (for example, the IMF; the solar wind velocity and pressure; or geomagnetic indices) which are directly related, in many cases with a physical basis, to disturbances in geospace. Such models are nonlinear dynamic systems (including prediction filters, linear and nonlinear) and neural networks. These relatively simple input-output algorithms are able to "learn" from a database of events how to represent a certain type of geospace activity. Modeling efforts have included the geomagnetic or ionospheric electric activity to solar wind and IMF changes (e.g., Valdivia et al., 1996; Vassiliadis et al., 1995; Weimer, 1996; Wu and Lundstedt, 1996); propagation of solar wind from one

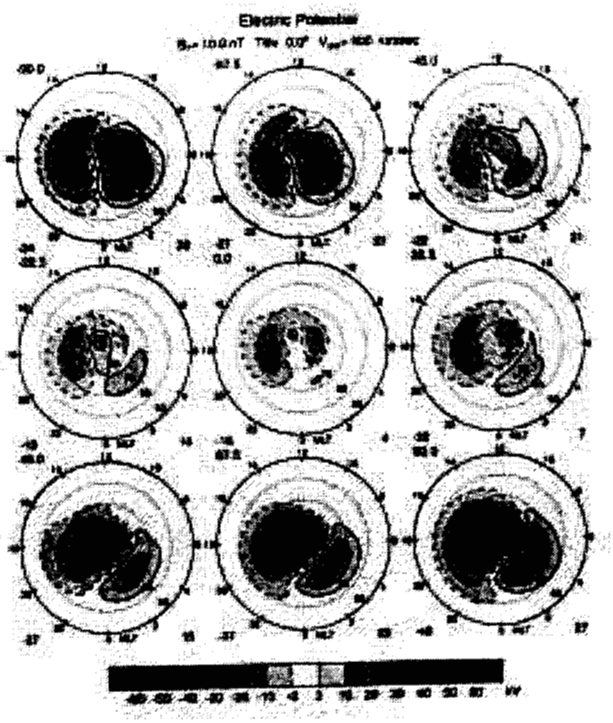

Fig. 9. The response of the high-latitude ionospheric electric potential to the interplanetary magnetic field (IMF) derived from DE-2 data for a specified solar wind input of constant amplitude, B = 10 nT, and variable clock angle (Weimer, 1996). The IMF clock angle is shown at the upper left corner in each graph, while the extreme positive and negative potentials in kV are shown at the lower left and right corners. Empirical models such as this will play a major role in the first phase of geospace forecasting.

region to another; and propagation of geomagnetic disturbances from one region to another (Vassiliadis et al., 1996). An example is shown in Fig. 9. Recently there have been several efforts to derive physically based models (Horton and Doxas, in press, 1997) and compare them with the empirical models; and derive time scales and strengths of the solar wind-magnetosphere-ionosphere coupling, from nonlinear filters (Klimas et al., this volume, 1998) or neural networks (Wray and Green, 1994).

But even with these early successes, space weather activities need mobilization and support at the government agency level. For this reason, several U.S. agencies with activities related to or affected by space weather conditions have coordinated their efforts through the National Space Weather Strategic and Implementation Plans (NSWC, 1995, 1997). At the same time individual agencies develop their own programs related to space weather. Both NOAA (through its Space Environment Center) and the Air Force have presented mechanisms for the transition of models to operations. NSF has initiated a series of workshops focused on specific problems due to space weather while NASA supports space weather activities through missions and research.

7.3 Recommendations for future development

There are standard requirements for a generic forecast, and in addition, there are specific modifications for each one of them for geospace forecasts. Standard requirements include timeliness, availability, and accuracy of the forecast. In our days the first one is accelerated by the rapid data distribution on the Internet.

The availability of geospace data is a critical factor for forecast quality. In addition to continuous monitoring of the solar photosphere, we need continuous solar wind monitoring by WIND and/or ACE to attain geomagnetic forecasting of 0.5–1 hour in advance. Funding new ideas of monitoring activity on the Sun and in geospace are necessary to widen the basis on which space weather can be built. On the ground we need denser coverage of the high-latitude ionospheric and geomagnetic response. Data compilation, storage, and rapid access become easier to handle with networks such as Intermagnet, CANOPUS, and IMAGE now available on line. Such databases have a twofold role: they are useful for empirical model development, and can aid real-time predictions; and they are useful for retrospective studies ("post-mortem" analyses) conducted by users (Kappenman and Livingston, in press, 1996).

Once models for geospace forecasting are developed, modern methods of validation need to be applied to measure model accuracy (Doggett, 1996). Only direct comparison of several models, or model families, on common data sets will display relative strengths and weaknesses. Standardization of forecasts and error analysis will improve the reliability of models.

For further progress under the present budget climate, interdisciplinary and intradisciplinary collaborations will have to increase in depth and scope. Currently several efforts in the magnetospheric and ionospheric groups are involved in linking empirical and physics-based models. One such case is the Space Weather Ionospheric Forecast Technologies effort, which combines models for geomagnetic index activity, high-latitude electric potentials (such as those of Fig. 9) and currents, to forecast ionospheric disturbances over northern geographic location (Siscoe and Maynard, 1996).

Finally, a preliminary outreach effort undertaken by several individual space physics groups and organizations, in conjunction with independent activities of the planetary physics community, has shown that the public is already interested in weather in space. In continuing and intensifying the outreach efforts, for example making the forecasts, especially those of large-scale events, and the related products widely accessible, we will raise the public's understanding of and support for space weather applications.

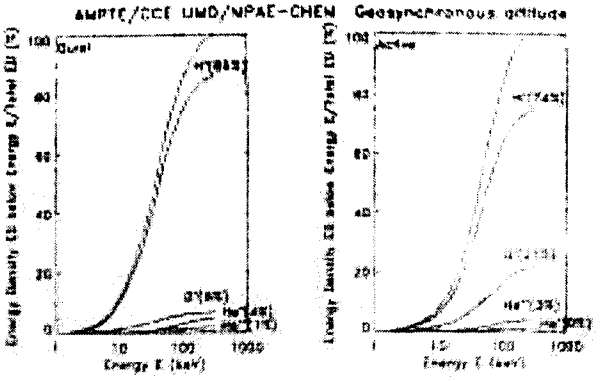

Fig. 10. Accumulated percentage of the ion energy density at geosynchronous altitude (i.e. outer ring current) as a function of energy Daglis et al. (1993). Plotted are curves for the total energy density as well as for the energy density of the 4 main ion species (H^+, O^+, He^{++}, He^+). The two panels show that both during quiet (left) and during active (right) times, the bulk of the plasma's energy density in the inner magnetosphere is contained in the energy range ~10-200 keV. More details in the text.

8 The terrestrial factor

8.1 The importance of the terrestrial ionosphere for geospace dynamic processes

It is beyond any doubt that the cause of all geospace activity is the entry of solar wind material and energy into the Earth magnetosphere. There is however a regulating factor that only gradually came to be considered by the scientific community: we refer to the terrestrial factor, which was more or less neglected during the first two decades of space research. There were two noteworthy exceptions: Dessler and Hanson (1961) and Axford (1970) suggested that the solar wind provides the energy for the magnetospheric processes (storms/substorms), while the particles are provided by the terrestrial ionosphere. Their suggestion remained without influence until the discovery of precipitating energetic O^+ ions by the Lockheed group in the early 1970s (Shelley et al., 1972).

The development of mass/charge-discriminating plasma instruments made it possible for numerous studies during the 1970s and the 1980s (e.g., Geiss et al., 1978; Peterson et al., 1981; Shelley et al., 1976; Strangeway and Johnson, 1984) to demonstrate that magnetospheric hot plasma contains a significant component of O^+. Eventually the well-founded and supported dominance of the solar wind as a particle source of the hot magnetospheric population was disputed. Following the confirmation of the significance of the ionospheric particle source, many studies (Baker et al., 1982; Cladis and Francis, 1992; Kaufmann and Lu, 1993; Lakhina, 1995; Moore, 1991; Rothwell et al., 1988; Young et al., 1981) on the influence of ionospheric-origin heavy ion species (He^+ and O^+) on magnetospheric dynamics were published. The influence of O^+ on wave growth, propagation, and decay is of special importance for magnetic storm dynamics (e.g., Singer et al., 1979; Thorne and Horne, 1997).

In the late 1980s, the AMPTE mission (Krimigis et al., 1982) complemented and extended the earlier studies with multi-species ion measurements extending into the higher ($\sim$ 20–200 keV/e) energy range. The missions Geos, ISEE 1 and ISEE 2, had covered only lower energies (<17 keV/e). The importance of full compositional measurements, extending to the higher (>20 keV) energy range cannot be overemphasized, since it has been shown that the bulk of the plasma's energy density in the near-Earth magnetosphere is contained in the energy range ~10-200 keV. Figure 10 (adopted from Daglis et al., 1993) shows both the contribution of the different ion species to the total energy density and the energy distribution of the ion energy density. The curves represent averages over 2.5 years of measurements by the CHEM instrument onboard AMPTE/CCE. They show the accumulated percentage of the ion energy density at geosynchronous altitude (i.e. outer ring current) as a function of energy. Plotted are curves for the total energy density as well as for the energy density of the 4 main ion species (H^+, O^+, He^{++}, He^+). The left panel shows the average energy density distribution in the outer ring current at geomagnetically quiet times, while the right panel shows it for active conditions. It is clear that the bulk of the total measured ion energy density is contained in the energy range ~10-200 keV. This fact is even more pronounced during magnetospheric dynamic processes such as storms and substorms (e.g., Daglis et al., 1994; Krimigis et al., 1985). Moreover, Daglis and Axford (1996) showed that the increase in

O^+ during substorms occurs predominantly in the upper energy range (>20 keV).

8.2 Ionospheric O^+ ions in substorms

Measurements with the CHEM spectrometer (Gloeckler et al., 1985) on board AMPTE/CCE provided important clues on the role of terrestrial origin ions (O^+ in particular) during substorms. Significant enhancements of O^+ ions during a substorm growth phase were shown by Daglis et al. (1990). A series of statistical studies based on CHEM measurements (e.g., Daglis et al., 1991a, 1993, 1994) demonstrated a strong correlation between the energy density of the ionospheric origin O^+ ions in the inner magnetotail, and the auroral electrojet activity during substorm expansion. This correlation was shown to exist at a time resolution of 15 min. Most of the previous studies had used long-time (usually several hours) averages of *AE* indices or the *Kp* index (e.g. Lennartsson and Sharp, 1985; Lennartsson and Shelley, 1986; Young et al., 1982). However, within a time interval of several hours, more than one substorms can take place and both the magnetospheric conditions and the ionospheric state can undergo a series of dramatic changes. The use of several-minute averages of measurements guarantees that the substorm features are not *a priori* smoothed out (Baker et al., 1986).

Daglis et al. (1996) used substorm observations with MICS (Magnetospheric Ion Composition Spectrometer, Wilken et al. (1992)) on board CRRES (Combined Release and Radiation Effects Satellite) to demonstrate that the O^+ abundance follows the intensity enhancements of the westward electrojet very closely in time, exhibiting a continuing increase, contrary to the behaviour of the other major ion species H^+ and He^{++}. An example is shown in Fig. 11. This feature, which is consistent with the above mentioned statistical studies of AMPTE/CCE observations (Daglis et al. (1994) and previous papers), points towards a fast activation of an extraction/acceleration mechanism which feeds the inner plasma sheet with ions of ionospheric origin during the substorm expansion. Gazey et al. (1996) showed that such substorm-time O^+ injections into the inner magnetosphere can originate in discrete auroral arcs. The study confirmed the importance of the auroral ionosphere, as already indicated by previous statistical studies (e.g., Daglis et al., 1994; Lockwood et al., 1985; Yau et al., 1984).

The ability of AMPTE/CCE and CRRES to acquire compositional measurements in the upper energy range permitted the recognition of the importance of ionospheric O^+ ions, because it is in the upper energy range where their contribution to the active magnetosphere is substantial. Motivated by the AMPTE/CCE and CRRES results, Daglis and Axford (1996) suggested that in response to increased solar wind-magnetosphere coupling a fast feeding of the magnetosphere with iono-

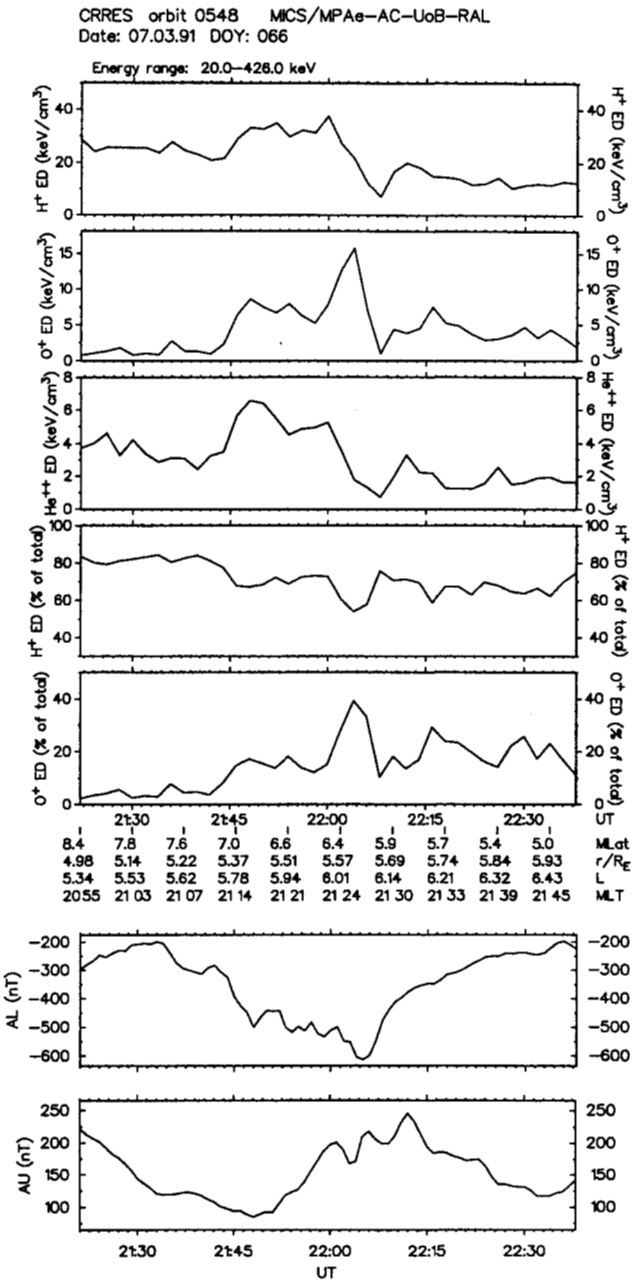

Fig. 11. Energy density time profile and provisional *AE* indices for a substorm observed by CRRES on 7 March 1991. The seven panels show: 1. the H^+ energy density (in keV/cm^3), 2. the O^+ energy density, 3. the He^{++} density, 4. the contribution of H^+ to the total energy density (in %), 5. the contribution of O^+ to the total energy density, 6. the *AL* index, 7. the *AU* index.

spheric ions can lead to a transient localized dominance of heavy ionospheric ions (namely O^+) and consequently to an ionospheric regulation (if not control) of the evolution of dynamic geospace processes. These results showed the capability of the auroral ionosphere to respond in a fast way (within characteristic substorm time scales) to energy input from the solar wind and the magnetosphere and to effectively load the near magnetotail with ions. Localized high abundance of O^+ ions can trigger substorm onset through the excitation of several kinds of instabilities, as described by a number of researchers (e.g., Baker et al., 1982; Büchner and Kuska, 1997; Cladis and Francis, 1992; Lakhina, 1995; Rothwell et al., 1988, 1994).

A high abundance of ionospheric ions in the plasma sheet may cause important differences between strings of multiple substorms and isolated substorms. There may be a feedback between increasingly high O^+ abundance and consecutive substorm expansion onsets. The first substorm in a series primes the ionospheric outflow, which in turn favors further substorm onsets through high concentrations of O^+. This procedure may be the key to the debated storm-substorm relationship (e.g., Kamide, 1979; Kamide et al., 1997a; Wolf et al., 1991). It is not clear if storm-time substorm occurrence influences ring current growth. Several researchers have argued that substorm occurrence is not essential to ring current growth (e.g., Iyemori and Rao, 1996; McPherron, 1997). However, it has been shown that intense storms have a dominant O^+ component near their maximum epoch (Daglis, 1997a), and the O^+ abundance is known to increase during substorm expansion (Daglis et al., 1992, 1994, 1996).

8.3 The ionospheric role in magnetic storm dynamics

CRRES observations of four intense and one moderate storm in 1991 (Daglis, 1997a) showed that $|Dst|$ and O^+ increase concurrently (see for example Fig. 12). Furthermore, O^+ was the dominant ion species at the maximum epoch of the intense storms (i.e. at highest $|Dst|$), as it was in the great February 1986 storm (Hamilton et al., 1988). Since the peaks in $|Dst|$ are due to the enhancement of the ring current, the CRRES observations actually show that the intensification of the ring current at storm maximum is mainly due to the contribution of O^+ ions. Taking into account that a fraction of H^+ (about 30% in the storm-time outer ring current) is also of ionospheric origin, it is clear that the majority of the ring current particles at storm maximum are of terrestrial origin. Inevitably three major questions emerge: 1. Do all intense storms have a dominant terrestrial ion component? 2. Is an intense ionospheric outflow a prerequisite of intense storms? 3. Is ring current decay regulated by the charge-exchange loss of energetic O^+ during the recovery of intense storms? The answer to these questions requires an extensive database of storm

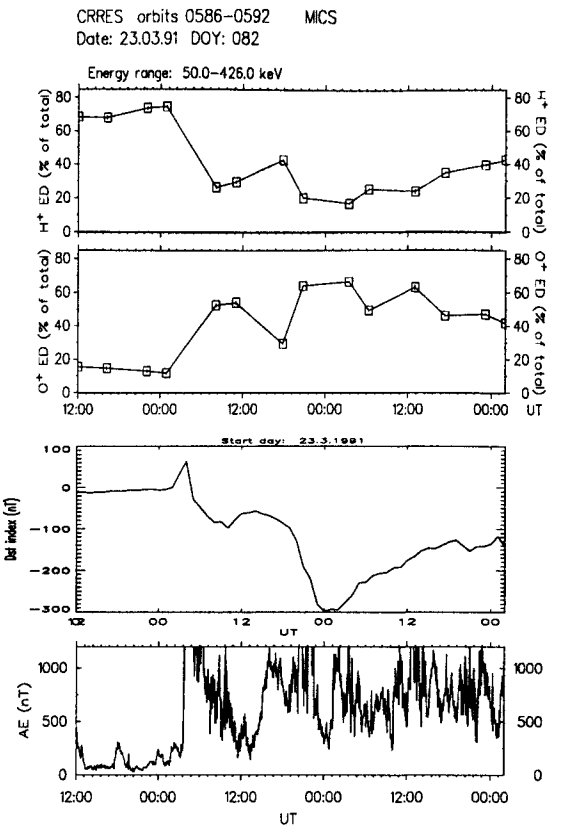

Fig. 12. The great magnetic storm of March 24, 1991. The diagram shows the time profile of the contribution of the two major ion species H^+ and O^+ to the total energy density of the energetic ion population in the outer ring current region L=5-7 (as measured by CRRES-MICS), and the time profiles of the *Dst* and *AE* indices. Squares with error bars mark the actual data points on the particle panels. The main features to be observed is the dominance of O^+ during storm maximum, as well as the concurrent increase of the $|Dst|$ level and of the O^+ contribution to the total ion energy density.

observations with full compositional measurements in the ring current, which unfortunately is not available at present, simply because AMPTE and CRRES are the only missions so far that have provided such measurements.

The great magnetic storm of March 24, 1991 (Fig. 12) with $|Dst|$ reaching peak values of more than 300 nT has been discussed by Daglis (1997a). The O^+ contribution to the total energy density in the outer ring current (L=5-7) was more than 65%. Fig. 12 demonstrates the concurrent O^+ and $|Dst|$ increase, as well as the fact that the O^+ contribution remains at an extraordinarily high level (above 40%) for a very extended time period (more than 30 hours). It should be noted that O^+ has a stronger earthward gradient than H^+, resulting in an earthward increase of the O^+ contribution. Over the L-range 5 to 6 for example, the O^+ contribution exceeds

75% (Daglis et al., submitted, 1998), which is 10% more than the average contribution in the L-range 5 to 7. These observations indicate that the ring current growth at the maximum epoch of the storm was due to the explosive enhancement of O^+ abundance.

The bottom panel of Fig. 12 shows the time profile of the preliminary *AE* index. It demonstrates the well known fact that the O^+ abundance and energy density in the inner plasma sheet increase during periods of enhanced auroral activity (e.g., Daglis et al., 1994). Furthermore, it indicates that a series of substorm expansions initiates and sustains the enhanced ionospheric feeding of the inner plasma sheet (Daglis and Axford, 1996), which leads to a rapid ultimate enhancement of the ring current, as observed during intense storms. It has been suggested that a feedback can develop between O^+ injections and substorm-breakups successively proceeding to the dusk-side and to lower *L*-shells (Baker et al., 1985; Rothwell et al., 1988). Such a feedback can drive a rapid enhancement of the ring current, since O^+ ions that are injected directly to the inner (L<6) midnight-duskside magnetosphere during substorm expansion (e.g., Kaye et al., 1981; Strangeway and Johnson, 1983) have a high probability to stay on closed drift paths and will quickly increase the ring current strength. Another piece of evidence comes from recent studies of DMSP measurements (Shiokawa and Yumoto, 1993), which showed that high-latitude field-aligned potential drops exhibit strong enhancements during the substorm recovery phase. Such potential drops are efficient agents of ionospheric ion acceleration, and they definitely increase the rate of ionospheric ion feeding of the inner plasma sheet during substorm recovery, especially in a series of successive substorms.

The March 24 storm exhibited a two-phase profile, both in *Dst* and in the level of O^+ contribution. Following the SSC (at 0341 UT) we can see an increase of the O^+ contribution from the ~10% level to the ~40% level, along with a drop of *Dst* to ~ −100 nT. A period of transient *Dst* recovery and O^+ decrease follows, and then we enter the maximum epoch of the storm, with both $|Dst|$ and O^+ reaching their peaks. A similar pattern in $|Dst|$ and O^+ was observed in the great storm of February 1986 (Hamilton et al., 1988). Intense magnetic storms often develop the two-step *Dst* profile (Tsurutani et al., 1988b). Kamide et al. (1997b) suggested that two-phase intense storms are actually double storms that occur subsequently and possibly owe their growth to different reasons. One of the possible scenarios is that two distinct processes play the leading role in the two successive *Dst* drops, that is the two successive enhancements of the ring current. The first enhancement of the ring current (first *Dst* drop) may be due to the magnetospheric convection driven by the southward IMF (e.g., McPherron, 1997), while the second ring current enhancement (second *Dst* drop) may be due to the substorm-associated accumulation of a new O^+ population.

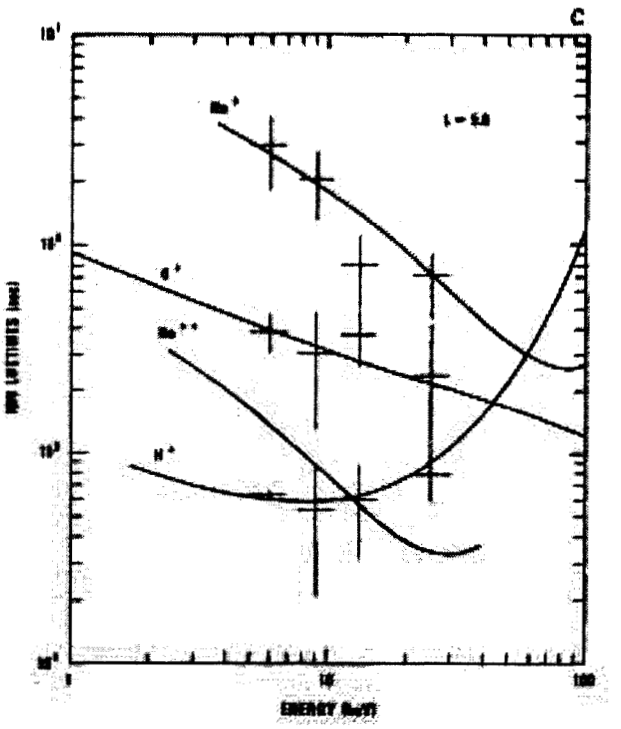

Fig. 13. Charge-exchange lifetimes of H^+, O^+, He^{++} and He^+ ions as a function of their energy for $L = 5$ (Smith et al., 1981).

An increased relative abundance of O^+ ions in the inner magnetosphere does not only have the effect of storm-time ring current enhancement. The resulting mass loading is important for wave growth, propagation and absorption (Kozyra et al., 1984; Moore, 1991; Singer et al., 1979; Thorne and Horne, 1994, 1997). Increased O^+ abundance also influences the decay rate of the ring current, since the charge-exchange lifetime of O^+ is considerably shorter than the H^+ lifetime for ring current energies (≥40 keV, see Fig. 13). This implies that O^+-dominated ring current will decay faster, at least initially. Such a fast initial ring current decay, associated with a large O^+ component during the storm main phase, has been indeed observed in the February 1986 storm (Hamilton et al., 1988), as well as in the storms of March 24, 1991, and of July 9, 1991 (Daglis, 1997a).

8.4 Conclusions

The importance of the terrestrial factor in solar-terrestrial coupling, and in storm and substorm dynamics in particular, has emerged from numerous studies with AMPTE and CRRES measurements. O^+, the major ion species outflowing from the terrestrial ionosphere, is a potential agent for triggering substorm onset, particularly in a series of substorms. The role of O^+ in storm dynam-

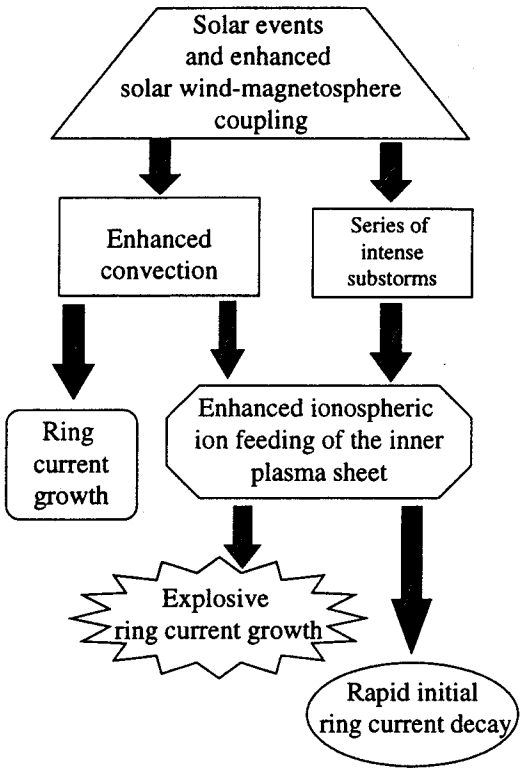

Fig. 14. The role of O^+, the major outflowing ionospheric ion, in the evolution of intense storms is twofold: 1. It causes the rapid final enhancement of the ring current at storm maximum, and 2. It induces an equally rapid initial ring current decay (Fig. 3 of Daglis, 1997b).

ics is twofold (see schematic diagram in Fig. 14): 1. Its explosive increase at storm maximum causes the rapid final enhancement of the ring current and the associated $|Dst|$, and 2. After the storm maximum, O^+ induces an equally rapid initial ring current decay (that is a rapid recovery of Dst), because its charge exchange lifetime is considerably short than that of H^+ at the ring current energies. In other words, the terrestrial plasma first provides the final touch and then drives the first (big) nail in the coffin of the ring current during the main phase of intense storms.

The major question emerging from these observations, i.e., if intense ionospheric outflow is a prerequisite and a regulator of intense storms, cannot be answered at present, because it requires an extensive database with full compositional measurements in the ring current during storms. Such a database does not exist yet. Under these conditions, every single case study is of special importance, and the ISTP opportunity is most useful. A diagnostic technique that can greatly advance our apprehension of storm and substorm dynamics is that of neutral atom imaging (e.g., Daglis and Livi, 1995; Roelof, 1989; Williams et al., 1992). The potential of this technique is discussed in detail in Section 9. Finally, an issue that deserves further attention is the relation of ionospheric outflow to particular solar events and interplanetary disturbances, such as CMEs, ICMEs and magnetic clouds (Daglis et al., 1997).

9 The potential of ENA imaging

9.1 ENA description and actual observations

One loss mechanism that has been suggested to account for the decay of ring current particle flux in the magnetosphere is charge-exchange with the neutral hydrogen of the exosphere. The outcome of this process consists in the so-called Energetic Neutral Atoms (ENA). These are atoms with energies of a few to hundreds of keV emitted from hot plasmas when energetic ions undergo charge-exchange interactions. The produced ENA leave the interaction region with essentially the same energy and direction of the incident ion (Fig. 15). The newly created ENA, no more affected by magnetic or electric fields, travel in a ballistic orbit, i.e. a straight line at these energies; it follows that the information of the originating ion is transferred far away from the ion location. Hence, we can interpret the ENAs as carriers of the hot plasma properties. Through unfolding procedures these properties can be easily reassembled, provided that the ENA are detected at a specific vantagepoint. In this way, the remote sensing of magnetospheric plasma becomes potentially possible. The success of this technique is constrained by two factors. First of all, in order to produce ENA, ions must interact with the exosphere gas: hence, this process does not work at distances $>\sim$ 10 R_E, where the exosphere gas density is too low. Secondly, the charge-exchange cross section is very small, so that only a tiny fraction of ions converts into ENA. It follows that this signal must be carefully discriminated with respect to other local ion signatures (see Orsini et al. (1994) for an exhaustive discussion on exosphere gas density and charge-exchange cross section) .

A first clear evidence of ENA emission from the geomagnetosphere came from the ion detectors on IMPs 7 and 8 and on ISEE-1 Roelof et al. (1985). When these satellites were located out of the magnetospheric hot plasma, energetic particles were detected to flow from the Earth direction. Roelof and Williams (1988) constructed the first ENA image of the terrestrial ring current using these data, thus giving credence to the possibility of remote sensing the planetary magnetospheres via ENA. After the pioneering incidental detection by ISEE-1, some other sporadic ENA observations have been reported by EPIC and HEP-LD instruments on board the GEOTAIL spacecraft (Lui et al., 1996; Wilken et al., 1997), and by PIPPI instrument on board the

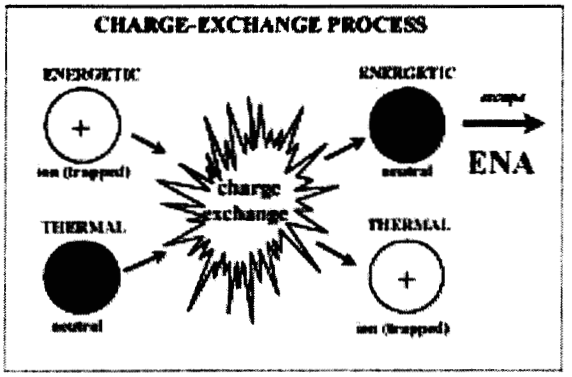

Fig. 15. Schematic representation of the charge-exchange mechanism: the energetic ion is neutralized, and escapes from the source location with unchanged energy and flow direction.

Swedish satellite ASTRID (Barabash et al., 1994). Since 1996, another hot plasma detector, the IPS-CEPPAD experiment on POLAR is systematically collecting ENA each time the satellite is near the apogee (~9 R_E) in the northern polar cup, where energetic charged particles are not present. Henderson et al. (1997) show some ENA images collected during storm time as well as during substorm time. During the storm occurred on August 29, 1996, the instrument detected a ring of enhanced ENA emission encircling the Earth. Although the data presented are very preliminary, and in spite of the coarse angular resolution and low efficiency (this instrument was not specifically designed for detecting ENA), the great potential of this technique is evident from the color plates.

9.2 ENA at low-altitude vantage points

Orsini et al. (1994) show that ENA could be monitored even from low-altitude vantage points, located at altitudes above 400-500 km; below this limit ENA start interacting significantly with the exosphere particles, so that the source ion energy and direction information is lost (De Michelis and Orsini, 1997). The advantage of ENA detection from low-altitude vantage points comes from the fact that imaging of specific regions is gained with great detail. Furthermore, any secondary ENA coming from further interaction with the Earth's atmosphere, below the vantagepoint, can be easily discriminated from the useful information coming from regions located above the vantagepoint. The expected ENA fluxes at low altitudes have been simulated by Orsini et al. (1994), by using the AMPTE/CCE-CHEM experiment data as input source (Gloeckler et al., 1985). During quiet periods, the estimated hydrogen ENA fluxes originating from the magnetic equatorial plane (integrated between 3 and 9 Earth radii) range between 5×10^2 $[cm^2\ s\ sr\ keV]^{-1}$ at 5 keV and 10^{-2} at 120 keV. Although the ring current O^+ ions are less abundant, the estimated oxygen ENA fluxes overcome the hydrogen fluxes at energies >80 keV . This is essentially due to the different profiles versus energy of the charge-exchange cross sections. During disturbed periods, the ion fluxes increase up to about one order of magnitude, especially at energies higher than 10 keV, and the expected ENA signal is expected to intensify significantly.

9.3 Focal points for magnetospheric research and ENA

The ENA spectra are strictly related to the source ion distributions; therefore, through signal unfolding procedures, it is possible to look globally at the magnetospheric ion populations. The necessary unfolding process is complicated by the fact that the ENA observed carry information of magnetospheric plasma weighted by the exosphere density and integrated along the line of sight from the vantagepoint to infinite. Image unfolding can be done on the basis of specific mathematical procedures (iterative forward modeling), which rely on iterative comparison of the actual images with model images until the differences are minimized (Roelof, 1987). This remote sensing technique preludes to new perspectives in the study of the planetary magnetosphere.

– *Global image of the plasma distribution in the Earth magnetosphere*

This objective is may be the most spectacular and implies a great educational potential. Up to now our capability to visualize geospace is limited to all that can emit or reflect electromagnetic radiation (for example: clouds, smokes and dust, rain, rainbows, auroras). The images one could obtain through ENA would enable to monitor a new class of phenomena linked to non-radiation emitting plasma. For example, it would be possible to visualize the evolution of phenomena like the plasma flow within the magnetospheric regions during magnetic storms and substorms Daglis and Livi (1995); Roelof (1987).

– *Space Weather*

This program was initiated in USA by the National Science Foundation (Division of Atmospheric Science) and its target is to do forecasts of interplanetary perturbations potentially dangerous for telecommunication systems, electronic apparatus on board satellites, flights on polar routes, etc. ENA instruments, giving global images, are among the most effective supports for the program. In fact, the study of the time relationship linking the various magnetospheric phenomena will allow a better understanding of the perturbation propagation.

– *ENA interaction with the Earth Atmosphere*

Below 450 km ENA start to react with the atmospheric gas and, because of elastic and non-elastic interactions,

are partly absorbed and partly reflected to the space (De Michelis and Orsini, 1997). Where the reflection rate is high, a true ENA "albedo" would become observable (E. C. Roelof, private communication, 1997).

– *Mechanisms of plasma loss of the ring current*

One of the major mechanisms of plasma loss of the ring current is charge-exchange (e.g., Jordanova et al., 1996). Good measurements of ENA fluxes can provide a better estimate of plasma losses. Moreover, they can provide an estimate of the variations of plasma losses as a function of geomagnetic activity.

– *Magnetospheric response to solar wind changes*

When the southward component of the interplanetary magnetic field and the solar wind speed increase, stresses in the magnetopause are generated that in turn generate field aligned currents that connect the magnetopause to the ionosphere (the so-called dayside region-1 currents). Through the region called "polar cap", these aligned currents propagate within the inner magnetosphere, setting a new currents system, named region-2 currents (Schield et al., 1969). Plasma pressure gradients are associated to this currents system, particularly in the ring current and in the plasma sheet. ENA measurements, depending on the plasma intensity fluxes in these regions, would allow the computation of the current density and the study of its space-time behavior.

– *Plasma injection in the ring current and convection electric field*

The plasma of the solar wind and of the ionosphere is injected in the inner magnetospheric field lines in the Polar Regions, through acceleration processes due to instability phenomena. This plasma then flows along the magnetic field lines, away from the Earth in the geomagnetic tail. The enhancements of the magnetic field and the dawn-dusk cross-tail electric field are the cause of drift movements that lead the plasma towards the equator, taking it back towards the Earth, up to the supplying the ring current. The ring current ions injected from the plasma sheet by the magnetic field gradient and by the E×B drift, move along the equipotential surface:

$$W = \mu B_m + qU = const \qquad (1)$$

where W is the total energy, $\mu = \frac{mv_\perp^2}{2B}$ is the magnetic moment, $v_\perp$ is the normal velocity, B_m is the mirror point magnetic field, q is the charge and U is the electric potential (Whipple Jr., 1978). Fig. 16 shows the electric equipotential contours on the equatorial magnetosphere. From equation (1) it follows that in the dusk sector, where U is lower, the adiabatic heating of the source ion distributions would influence the ENA spectra. Conversely, in the dawn sector the ENA signal would reflect the cooling of the ion spectra (Fig. 16).

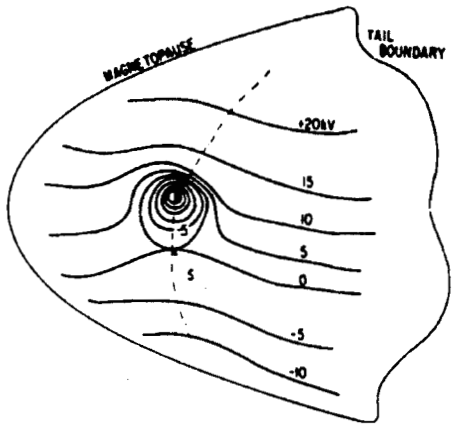

Fig. 16. A typical equipotential pattern in the magnetosphere showing an approximately uniform cross-tail field far from the Earth and the coronation field near the Earth. The dashed curve is the locus of points where the magnetic field is either a maximum or a minimum in any given equipotential (Fig. 1 from Whipple Jr. (1978)).

Milillo et al. (1996) simulate the ENA energy spectra by using the AMPTE/CCE-CHEM ion distributions as source for the simulation. The modeled ENA - derived along both dawn and dusk look directions (Fig. 17) are roughly unfolded in order to reconstruct the ion velocity distribution function at 90° pitch angle.

By comparing the unfolded ion spectra, the relative variation of the ion kinetic energy is derived, thus allowing an estimate of the electric potential drop ΔU. Milillo et al. (1996) conclude that the evolution of the convection electric field could be continuously and globally monitored via ENA detection. .

9.4 Clues for future magnetospheric missions

Actually, ENA data are not yet available, except for a few sporadic events and the recent data coming from IPS-CEPPAD on POLAR. Nevertheless, the observations reported as well as the simulation efforts have already confirmed the great potential of such measurements for global understanding of the magnetospheric plasma processes. More data, systematically collected by instruments fully devoted to ENA detection, are needed. For these reasons, a global imaging mission named IMAGE (Burch, 1996) is planned to be launched at the beginning of 2000. This mission will carry three ENA imagers, operating at three distinct energy ranges, between a few eV and hundreds of keV. An effort for providing other satellites (to be launched in the same period of IMAGE) with ENA instrumentation on board would be worth: in fact, multi-spacecraft ENA imaging would allow three-dimensional stereographic analyses of the inner magnetosphere. We are convinced that ENA detection will constitute an unprecedented opportunity for a global understanding of plasma dynamics in the

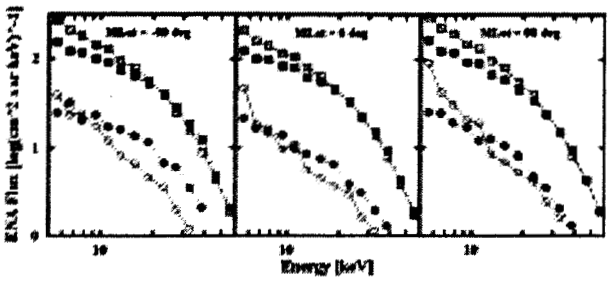

Fig. 17. Comparisons of the ENA H (squares) and O (circles) spectra simulated for the dawn (white) and dusk (black) directions, respectively at +22.5° and -22.5° from the Sun-Earth axis. The three panels refer to three different vantage points (at MLT = 0000), with magnetic latitudes Mlat = -50°, 0°, and +50°.

Earth's magnetosphere.

10 Conclusion

Solar-terrestrial coupling is multifaceted just as are the physical systems it involves. Disturbances originating at the Sun and traveling through interplanetary space induce explosive processes such as storms and substorms in geospace. Basic research of solar-terrestrial physics has long been most attractive. Recently, solar-terrestrial physics acquired an applied touch too, due to the often-deleterious effects of solar-terrestrial coupling processes on technological systems (e.g., Baker et al., 1994; Lanzerotti, 1994), due to increasing indications that solar induced geomagnetic disturbances may be hazardous for human health (e.g., Halberg et al., 1991; Roederer, 1995; Watanabe et al., 1994), and due to considerations on the influence of solar wind on weather and climate change (e.g., Tinsley, 1994).

The most application-oriented part of solar-terrestrial research today is space weather forecasting, which is an effort to have "visible" (and useful to the technological society) means of predicting major geospace disturbances. This new aspect of research in our field should be given proper attention and support. Certainly it cannot develop without more detailed input regarding differences in solar-terrestrial coupling due to the variations in solar wind composition (Section 3), the geoeffectiveness of different interplanetary structures (Section 4), the differences in plasma transfer processes at the magnetopause (Section 5), the dynamics of substorms (Section 6), the regulative role of the terrestrial ionosphere (Section 8), or the radiation belt dynamics (an important topic that has not been covered by this paper). New measuring techniques (Section 9) are essential to the effort for more global information, since a holistic approach is necessary in order to put pieces together and obtain a comprehensive picture of solar-terrestrial processes.

Finally, meetings like the Symposium on Solar-Terrestrial Coupling Processes in Paros, which bring together scientists working on different topical fields, have the merit of promoting fertile interaction, of providing overview on the advances of the "foreign" fields of research, and of giving birth to new ideas on collaborations and future research directions.

Acknowledgements. Parts of this work were done at the Jet Propulsion Laboratory, California Institute of Technology, by Bruce Tsurutani under contract with NASA. The convenors of the Symposium on Solar-Terrestrial Coupling Processes would like to thank Manfred Scholer for efficient chairing of the Panel Session, and all the panel members for their excellent contributions.

References

Angelopoulos, V., Kennel, C. F., Coroniti, F. V., Pellat, R., Kivelson, M. G., Walker, R. J., Russell, C. T., Baumjohann, W., Feldman, W. C., and Gosling, J. T., Statistical characteristics of bursty bulk flow events, *J. Geophys. Res.*, *99*, 21,257–21,280, 1994.

Axford, W. I., On the origin of radiation belt and auroral primary ions, in *Particles and Field in the Magnetosphere*, edited by B. M. McCormac, pp. 46–59, D. Reidel, Norwell, Mass., 1970.

Baker, D. N., E. W. Hones Jr., Young, D. T., and Birn, J., The possible role of ionospheric oxygen in the initiation and development of plasma sheet instabilities, *Geophys. Res. Lett.*, *9*, 1337–1340, 1982.

Baker, D. N., Fritz, T. A., Lennartsson, W., Wilken, B., Kroehl, H. W., and Birn, J., The role of heavy ions in the localization of substorm disturbances on March 22, 1979: CDAW 6, *J. Geophys. Res.*, *90*, 1273–1281, 1985.

Baker, D. N., Bargatze, L. F., and Zwickl, R. D., Magnetospheric response to the IMF: substorms, *J. Geomagn. Geoelectr.*, *38*, 1047–1073, 1986.

Baker, D. N., Kanekal, S., Blake, J. B., Klecker, B., and Rostoker, G., Satellite anomalies linked to electron increase in the magnetosphere, *Eos Trans. AGU*, *75* (35), 401–405, 1994.

Baker, D. N., Pulkkinen, T. I., Angelopoulos, V., Baumjohann, W., and McPherron, R. L., Neutral line model of substorms: Past results and present view, *J. Geophys. Res.*, *101*, 12,975–13,010, 1996.

Bame, J., Asbridge, J., Feldman, W., and Gosling, J., Evidence for a structure-free state at high solar wind speeds, *J. Geophys. Res.*, *82*, 1487–1492, 1977.

Barabash, S., Lundin, R., Norberg, O., Chase, C., Mauk, B., and Roelof, E., The Swedish microsatellite ASTRID: a first attempt at global magnetospheric imaging, *Eos Trans. AGU, Fall Meet. Suppl.*, *75*, 546, 1994.

Baumjohann, W., The near-Earth plasma sheet: An AMPTE/IRM perspective, *Space Sci. Rev.*, *64*, 141–163, 1993.

Baumjohann, W., Kamide, Y., and Nakamura, R., Substorms, storms, and the near-earth tail, *J. Geomagn. Geoelectr.*, *48*, 177–185, 1996.

Büchner, J. and Kuska, J. P., On the possible influence of oxygen ions on the stability of the magnetotail current sheet, Paper presented at the 8th Scientific Assembly of IAGA Uppsala, Sweden, August 4-15. Book of abstracts, p. 271, 1997.

Burch, J. L., IMAGE overview, *Eos Trans. AGU, Fall Meet. Suppl.*, *77*, F564, 1996.

Burlaga, L. F., Behannon, K. W., Hansen, S. F., Pneuman, G. W., and Feldman, W. C., Sources of magnetic fields in recurrent interplanetary streams, *J. Geophys. Res.*, *83*, 4177, 1978.

Burlaga, L. F., Sittler, E., Mariani, F., and Schwenn, R., Magnetic loop behind an interplanetary shock: Voyager, Helios, and IMP-8 observations, *J. Geophys. Res.*, *86*, 6673, 1981.

Caan, M. N., McPherron, R. L., and Russell, C. T., Solar wind and substorm related changes in the lobes of the geomagnetic tail, *J. Geophys. Res.*, *78*, 8087, 1973.

Caan, M. N., McPherron, R. L., and Russell, C. T., Substorm and interplanetary magnetic field effects on the geomagnetic tail lobes, *J. Geophys. Res.*, *80*, 191–194, 1975.

Cladis, J. B. and Francis, W. E., Distribution in magnetotail of O^+ ions from cusp/cleft ionosphere: A possible substorm trigger, *J. Geophys. Res.*, *97*, 123–130, 1992.

Cowley, S. W. H., The causes of convection in the Earth's magnetosphere: A review of developments during IMS, *Rev. Geophys.*, *20*, 531, 1982.

Daglis, I. A., The role of magnetosphere-ionosphere coupling in magnetic storm dynamics, in *Magnetic Storms, Geophys. Monogr. Ser.*, vol. 98, edited by B. T. Tsurutani, W. D. Gonzalez, Y. Kamide, and J. K. Arballo, pp. 107–116, AGU, Washington, D. C., 1997a.

Daglis, I. A., Terrestrial agents in the realm of space storms: Missions study oxygen ions, *Eos Trans. AGU*, *24*, 245–251, 1997b.

Daglis, I. A. and Axford, W. I., Fast ionospheric response to enhanced activity in geospace: Ion feeding of the inner magnetotail, *J. Geophys. Res.*, *101*, 5047–5065, 1996.

Daglis, I. A. and Livi, S., Merits for substorm research from imaging of charge-exchange neutral atoms, *Ann. Geophys.*, *13*, 505–516, 1995.

Daglis, I. A., Sarris, E. T., and Kremser, G., Indications for ionospheric participation in the substorm process from AMPTE/CCE observations, *Geophys. Res. Lett.*, *17*, 57–60, 1990.

Daglis, I. A., Paschalidis, N. P., Sarris, E. T., Axford, W. I., Kremser, G., Wilken, B., and Gloeckler, G., Statistical features of the substorm expansion-phase as observed by AMPTE/CCE, in *Magnetospheric Substorms, Geophys. Monogr. Ser.*, vol. 64, edited by J. R. Kan, T. A. Potemra, S. Kokubun, and T. Iijima, pp. 323–332, AGU, Washington, D. C., 1991a.

Daglis, I. A., Sarris, E. T., and Kremser, G., Ionospheric contribution to the cross-tail current during the substorm growth phase, *J. Atmos. Terr. Phys.*, *53*, 1091–1098, 1991b.

Daglis, I. A., Sarris, E. T., Kremser, G., and Wilken, B., On the solar wind-magnetosphere-ionosphere coupling: AMPTE/CCE particle data and the *AE* indices, in *Study of the Solar-Terrestrial System, ESA SP-346*, edited by R. Reinhard and J. J. Hunt, pp. 193–198, European Space Agency, Paris, 1992.

Daglis, I. A., Sarris, E. T., and Wilken, B., AMPTE/CCE CHEM observations of the ion population at geosynchronous altitudes, *Ann. Geophys.*, *11*, 685–696, 1993.

Daglis, I. A., Livi, S., Sarris, E. T., and Wilken, B., Energy density of ionospheric and solar wind origin ions in the near-Earth magnetotail during substorms, *J. Geophys. Res.*, *99*, 5691–5703, 1994.

Daglis, I. A., Axford, W. I., Livi, S., Wilken, B., Grande, M., and Søraas, F., Auroral ionospheric ion feeding of the inner plasma sheet during substorms, *J. Geomagn. Geoelectr.*, *48*, 729–739, 1996.

Daglis, I. A., Axford, W. I., Sarris, E. T., Livi, S., and Wilken, B., Particle acceleration in geospace and its association with solar events, *Sol. Phys.*, *172*, 287–296, 1997.

Daglis, I. A., Kamide, Y., Sarris, E. T., and Wilken, B., Ring current evolution during the great geomagnetic storm of March 1991, *J. Geophys. Res.*, submitted, 1998.

De Michelis, P. and Orsini, S., Energetic neutral atoms propagating toward the Earth: Analysis of the reduction rate due to ionospheric and atmospheric interactions, *J. Geophys. Res.*, *102*, 185–194, 1997.

Dessler, A. J. and Hanson, W. B., Possible energy source for the aurora, *Astrophys. J.*, *134*, 1024–1025, 1961.

Doggett, K. A., *The Evaluation of Space Weather Forecasts.* Proceedings of a Workshop at Boulder, Colorado, June 19-21, 1996, NOAA/SEC, Boulder, CO, 1996.

Dungey, J. W., Interplanetary magnetic field and the auroral zones, *Phys. Rev. Letters*, *6*, 47–48, 1961.

Freeman, J. W., Nagai, A., Reiff, P., Denig, W., Gussenhoven-Shea, S., Heinemann, M., Rich, F., and Hairston, M., The use of neural networks to predict magnetospheric parameters for input to a magnetospheric forecast model, in *Artificial Intelligence Applications in Solar Terrestrial Physics*, edited by J. Joselyn, H. Lundstedt, and J. Trollinger, pp. 167–181, NOAA, Boulder, 1994.

Fuselier, S. A., Anderson, B. A., and Onsager, T. G., Particle signatures of magnetic topology at the magnetopause: AMPTE/CCE observations, *J. Geophys. Res.*, *100*, 11,805, 1995.

Garrard, T. L. and Stone, E. C., Composition of energetic particles from solar flares, *Adv. Space Res.*, *14* (10), 589–598, 1994.

Gazey, N. G. J., Lockwood, M., Grande, M., Perry, C. H., Smith, P. N., Coles, S., Aylward, A. D., Bunting, R. J., Opgenoorth, H., and Wilken, B., EISCAT/CRRES observations: Nightside ionospheric ion outflow and oxygen-rich substorm injections, *Ann. Geophys.*, *14*, 1032–1043, 1996.

Geiss, J. and Young, D. T., Production and transport of O^{++} in the ionosphere and plasmasphere, *J. Geophys. Res.*, *86*, 4739–4750, 1981.

Geiss, J., Balsiger, H., Eberhardt, P., Walker, H. P., Weber, L., Young, D. T., and Rosenbauer, H., Dynamics of magnetospheric ion composition as observed by the GEOS mass spectrometer, *Space Sci. Rev.*, *22*, 537–566, 1978.

Geiss, J., Gloeckler, G., von Steiger, R., Balsiger, H., Fisk, L. A., Galvin, A. B., Ipavich, F. M., Livi, S., McKenzie, J. F., Ogilvie, K. W., and Wilken, B., The southern high-speed stream: Results from the SWICS instrument on Ulysses, *Science*, *268*, 1033–1036, 1995.

Gloeckler, G., Ion composition measurement techniques for space plasmas, *Rev. Sci. Instrum.*, *61*, 3613–3620, 1990.

Gloeckler, G., Ipavich, F. M., Stüdemann, W., Wilken, B., Hamilton, D. C., Kremser, G., Hovestadt, D., Gliem, F., Lundgren, R. A., Rieck, W., Tums, E. O., Cain, J. C., MaSung, L. S., Weiss, W., and Winterhoff, H. P., The charge-energy-mass (CHEM) spectrometer for 0.3 to 300 keV/*e* ions on the AMPTE/CCE, *IEEE Trans. Geosci. Remote Sens.*, *GE-23*, 234–240, 1985.

Gloeckler, G., Ipavich, F. M., Hamilton, D. C., Wilken, B., and Kremser, G., Heavy ion abundances in coronal hole solar wind flows (abstract), *Eos Trans. AGU*, *70*, 424, 1989.

Gonzalez, W. D. and Tsurutani, B. T., Criteria of interplanetary parameters causing intense magnetic storms ($Dst < -100$nT), *Planet. Space Sci.*, *35*, 1101–1109, 1987.

Gosling, J. T., Thomsen, M. F., Bame, S. J., Onsager, T. G., and Russell, C. T., The electron edge of the low-latitude boundary layer during accelerated flow events, *Geophys. Res. Lett.*, *17*, 1833, 1990.

Grande, M., Perry, C. H., Blake, J. B., Chen, M. W., Fennell, J. F., and Wilken, B., Observations of iron, silicon, and other heavy ions in the geostationary altitude region during late March 1991, *J. Geophys. Res.*, *101*, 24707, 1996.

Haerendel, G., Microscopic plasma processes related to reconnection, *J. Atmos. Terr. Phys.*, *40*, 341, 1978.

Haerendel, G., Disruption, ballooning, or auroral avalanche: On the cause of substorms, in *Substorms 1, ESA SP-335*, pp. 417–420, European Space Agency, Paris, 1992.

Halberg, F., Breus, T. K., Cornélissen, G., Bingham, C., Hillman,

D. C., Rigatuso, J., Delmore, P., and Bakken, E., *Chronobiology in Space*, Univ. of Minnesota, Minneapolis, MN, 1991.

Hamilton, D. C., Gloeckler, G., Ipavich, F. M., Stüdemann, W., Wilken, B., and Kremser, G., Ring current development during the great geomagnetic storm of February 1986, *J. Geophys. Res.*, *93*, 14,343–14,355, 1988.

Henderson, M. G., Reeves, G. D., Spence, H. E., Sheldon, R. B., Jorgensen, A. M., Blake, J. B., and Fennell, J. F., First energetic neutral atom images from Polar, *Geophys. Res. Lett.*, *24*, 1167–1170, 1997.

Henoux, J.-C. and Somov, B., First ionisation potential fractionation, in *Coronal Streamers, Coronal Loops, and Coronal and Solar Wind Composition, ESA SP-348*, pp. 325–330, European Space Agency, Paris, 1992.

Hoeksema, J. T. and Zhao, X. P., Prediction of magnetic orientation in $-B_z$ events, *J. Geophys. Res.*, *97*, 3151, 1992.

Horton, W. and Doxas, I., A low-dimensional dynamical model for the solar wind driven geotail-ionosphere system, *J. Geophys. Res.*, *102*, in press, 1997.

Huber, M. C. E., Foukal, P. V., Noyes, R. W., Reeves, E. M., Schmahl, E. J., Timothy, J. G., Vernazza, J. E., and Withbroe, G. L., Extreme-ultraviolet observations of coronal holes: Initial results from SKYLAB, *Astrophys. J. (Letters)*, *194*, 115–118, 1974.

Iyemori, T. and Rao, D. R. K., Decay of the Dst field of geomagnetic disturbance after substorm onset and its implication to storm - substorm relation, *Ann. Geophys.*, *14*, 608–618, 1996.

Jordanova, V. K., Kistler, L. M., Kozyra, J. U., Khazanov, G. V., and Nagy, A. F., Collisional losses of ring current ions, *J. Geophys. Res.*, *101*, 111, 1996.

Kamide, Y., Relationship between substorms and storms, in *Dynamics of the magnetosphere*, edited by S.-I. Akasofu, pp. 425–443, D. Reidel, Dordrecht, 1979.

Kamide, Y., Baumjohann, W., Daglis, I. A., Gonzalez, W. D., Grande, M., Joselyn, J. A., McPherron, R. L., Phillips, J. L., Reeves, G. D., Rostoker, G., Sharma, A. S., Singer, H. J., Tsurutani, B. T., and Vasyliunas, V. M., Current understanding of magnetic storms: Storm/substorm relationships, *J. Geophys. Res.*, submitted, 1997a.

Kamide, Y., Yokoyama, N., Gonzalez, W. D., Tsurutani, B. T., Daglis, I. A., Brekke, A., and Masuda, S., Two-step develoment of geomagnetic storms, *J. Geophys. Res.*, in press, 1997b.

Kan, J. R., A theory of patchy and intermittent reconnection for magnetospheric flux transfer events, *J. Geophys. Res.*, *93*, 5613, 1988.

Kappenman, J. G. and Livingston, J. G., An analysis of GSU transformer failure rates and possible association with geomagnetic disturbances, in *NRL National Space Weather Workshop*, edited by S. Antiochos, ONR, in press, 1996.

Kasotakis, G., Sarris, E. T., Marhavilas, P., Sidiropoulos, N. F., Trochoutsos, P., Daglis, I. A., and Dialetis, D., Variations in the ratio of particle to magnetic field energy density, as observed by Ulysses/HI-SCALE, *Phys. Chem. Earth*, this volume, 1997.

Kaufmann, R. L. and Lu, C., Cross-tail current: resonant orbits, *J. Geophys. Res.*, *98*, 15,447–15,465, 1993.

Kaye, S. M., Johnson, R. G., Sharp, R. D., and Shelley, E. G., Observations of transient H^+ and O^+ bursts in the equatorial magnetosphere, *J. Geophys. Res.*, *86*, 1335–1344, 1981.

Kennel, C. F., Edmiston, J. P., and Hada, T., A quarter century of collisionless shock research, in *Collisionless Shocks in the Heliosphere: A Tutorial Review, Geophys. Monogr. Ser.*, vol. 34, edited by R. G. Stone and B. T. Tsurutani, p. 1, AGU, Washington, D. C., 1985.

Klimas, A. J., Vassiliadis, D., and Baker, D. N., Data-derived analogues of the solar wind-magnetosphere interaction, *Phys. Chem. Earth*, this volume, 1998.

Kozyra, J. U., Cravens, T. E., Nagy, A. F., Fontheim, E. G., and Ong, R. S. B., Effects of energetic heavy ions on electromagnetic ion cyclotron wave generation in the plasmapause region, *J. Geophys. Res.*, *89*, 2217–2233, 1984.

Krimigis, S. M., Carbary, J. F., Keath, E. P., Bostrom, C. O., Axford, W. I., Gloeckler, G., Lanzerotti, L. J., and Armstrong, T. P., Characteristics of hot plasma in the Jovian magnetosphere: Results from the Voyager spacecraft, *J. Geophys. Res.*, *86*, 8227–8257, 1981.

Krimigis, S. M., Haerendel, G., McEntire, R. W., Paschmann, G., and Bryant, D. A., The active magnetospheric particle tracer explorers (AMPTE) program, *Eos Trans. AGU*, *63*, 843–850, 1982.

Krimigis, S. M., Gloeckler, G., McEntire, R. W., Potemra, T. A., Scarf, F. L., and Shelley, E. G., Magnetic storm of September 4, 1984: A synthesis of ring current spectra and energy densities measured with AMPTE/CCE, *Geophys. Res. Lett.*, *12*, 329–332, 1985.

Lakhina, G. S., Excitation of plasma sheet instabilities by ionospheric O^+ ions, *Geophys. Res. Lett.*, *22*, 3453–3456, 1995.

Lanzerotti, L. J., Impacts of solar-terrestrial processes on technological systems, in *Solar-Terrestrial Energy Program, COSPAR Colloquia Series Vol. 5*, edited by D. N. Baker, V. O. Papitashvili, and M. J. Teague, pp. 547–555, Pergamon Press, London, 1994.

Lanzerotti, L. J., Armstrong, T. P., Maclennan, C. G., Simnett, G. M., Cheng, A. F., Gold, R. E., Thomson, D. J., Krimigis, S. M., Anderson, K. A., Hawkins, S. E., Pick, M., Roelof, E. C., Sarris, E. T., and Tappin, S. J., Measurements of hot plasma in the magnetosphere of Jupiter, *Planet. Space Sci.*, *41*, 893–917, 1993.

Lee, L. C. and Fu, Z. F., A theory of magnetic flux transfer at the Earth's magnetopause, *Geophys. Res. Lett.*, *12*, 105, 1985.

Lennartsson, W. and Sharp, R. D., Relative contributions of terrestrial and solar wind ions in the plasma sheet, *Adv. Space Res.*, *5* (4), 411–414, 1985.

Lennartsson, W. and Shelley, E. G., Survey of 0.1- to 16-keV/*e* plasma sheet ion composition, *J. Geophys. Res.*, *91*, 3061–3076, 1986.

Lockwood, M., J. H. Waite Jr., Moore, T. E., Johnson, J. F. E., and Chappell, C. R., A new source of suprathermal O^+ near the dayside polar cap boundary, *J. Geophys. Res.*, *90*, 4099–4116, 1985.

Lui, A. T. Y., McEntire, R. W., and Krimigis, S. M., Evolution of the ring current during two geomagnetic storms, *J. Geophys. Res.*, *92*, 7459–7470, 1987.

Lui, A. T. Y., Lopez, R. E., Krimigis, S. M., McEntire, R. W., Zanetti, L. J., and Potemra, T. A., A case study of magnetotail current sheet disruption and diversion, *Geophys. Res. Lett.*, *15*, 721–724, 1988.

Lui, A. T. Y., Williams, D. J., Roelof, E. C., McEntire, R. W., and Mitchell, D. G., First composition measurements of energetic neutral atoms, *Geophys. Res. Lett.*, *23*, 2641–2644, 1996.

McPherron, R. L., The role of substorms in the generation of magnetic storms, in *Magnetic Storms, Geophys. Monogr. Ser.*, vol. 98, edited by B. T. Tsurutani, W. D. Gonzalez, Y. Kamide, and J. K. Arballo, pp. 131–147, AGU, Washington, D. C., 1997.

Milillo, A., Orsini, S., Daglis, I. A., and Candidi, M., Ring current ion flows and convection electric field as expected from observations by SAC-B/ISENA, *Geophys. Res. Lett.*, *23*, 3285–3288, 1996.

Mish, W. H., Acuna, M. H., and Ogilvie, K. W., The Global Geospace Science program and its investigations, *Space Sci. Rev.*, *71*, 5, 1995.

Moore, T. E., Origin of magnetospheric plasma, *U.S. Natl. Rep. Int. Union Geod. Geophys. 1987-1991, Rev. Geophys.*, *29*, 1039–1048, 1991.

Nagai, T. and Machida, S., Magnetic reconnection in the near-earth tail, in *New Perspectives of the Earth Magnetotail, Geophys. Monogr. Ser.*, edited by A. Nishida and D. N. Baker,

AGU, Washington, D. C., in press, 1997.

Nishida, A., Can random reconnection on the magnetopause produce the low-latitude boundary layer?, *Geophys. Res. Lett.*, *16*, 227, 1989.

Nishida, A., Mukai, T., Yamamoto, T., Saito, Y., and Kokubun, S., Magnetotail convection in geomagnetically active times, 1. distance to the neutral lines, *J. Geomagn. Geoelectr.*, *48*, 489–401, 1996.

NSWC, The National Space Weather Program: The Strategic Plan, *Office of the Federal Coordinator for Meteorological Services and Supporting Research, FCM-P30-1995*, 1995.

NSWC, The National Space Weather Program: The Implementation Plan, *Office of the Federal Coordinator for Meteorological Serv ices and Supporting Research, FCM-P31-1997*, 1997.

Ogino, T., Walker, R. J., and Ashour-Abdalla, M., A magnetohydrodynamic simulation of the formation of magnetic flux tubes at the Earth's dayside magnetopause, *Geophys. Res. Lett.*, *16*, 155, 1989.

Orsini, S., Daglis, I. A., Candidi, M., Hsieh, K. C., Livi, S., and Wilken, B., Model calculation of energetic neutral atoms precipitation at low altitudes, *J. Geophys. Res.*, *99*, 13,489–13,498, 1994.

Papadopoulos, K., Goodrich, C., Wiltberger, M., Lopez, R., and Lyon, J., The Physics of Substorms as Revealed by the ISTP, *Phys. Chem. Earth*, this volume, 1997.

Peterson, W. K., Sharp, R. D., Shelley, E. G., Johnson, R. G., and Balsiger, H., Energetic ion composition of the plasma sheet, *J. Geophys. Res.*, *86*, 761–767, 1981.

Poland, A., The Sun as never seen before, *Eos Trans. AGU*, *78*, 133, 1997.

Pu, Z. Y., Yei, M., and Liu, Z. X., Generation of vortex induced tearing mode instability at the magnetopause, *J. Geophys. Res.*, *95*, 10559, 1990.

Raeder, J., Walker, R. J., and Ashour-Abdalla, M., The structure of the distant geomagnetic tail during long periods of northward imf, *Geophys. Res. Lett*, *22*, 349, 1995.

Rezeau, L., Roux, A., and Russell, C. T., Characterization of small-scale structures at the magnetopause from ISEE measurements, *J. Geophys. Res.*, *98*, 179, 1993.

Roederer, J. G., Are magnetic storms hazardous to your health?, *Eos Trans. AGU*, *76*, 441–445, 1995.

Roelof, E. C., Energetic neutral atom image of a storm-time ring current, *Geophys. Res. Lett.*, *14*, 652–655, 1987.

Roelof, E. C., Remote sensing of the ring current using energetic neutral atoms, *Adv. Space Res.*, *9* (12), 195–203, 1989.

Roelof, E. C. and Williams, D. J., The terrestrial ring current: from in situ measurement to global images using energetic neutral atoms, *John Hopkins APL Techn. Dig.*, *9*, 144, 1988.

Roelof, E. C., Mitchell, D. G., and Williams, D. J., Energetic neutral atoms (E~50 keV) from the ring current: IMP 7/8 and ISEE 1, *J. Geophys. Res.*, *90*, 10,991–11,008, 1985.

Rothwell, P. L., Block, L. P., Silevitch, M. B., and Fälthammar, C.-G., A new model for substorm onsets: The pre-breakup and triggering regimes, *Geophys. Res. Lett.*, *15*, 1279–1282, 1988.

Rothwell, P. L., Silevitch, M. B., Block, L. P., and Fälthammar, C.-G., O^+ ions and substorm onsets, in *Proceedings of International Conference on Substorms 2, Fairbanks, U.S.A., March 7-11*, edited by J. R. Kan, J. D. Craven, and S.-I. Akasofu, pp. 591–594, Univ. of Alaska, Fairbanks, 1994.

Russell, C. T., The magnetopause, in *Physics of Magnetic Flux Ropes, Geophys. Monogr. Ser.*, vol. 58, edited by C. T. Russell, E. R. Priest, and L. C. Lee, p. 439, AGU, Washington, D. C., 1990.

Russell, C. T. and Elphic, R. C., Initial ISEE magnetometer results: magnetopause observations, *Space Sci. Rev.*, *22*, 691, 1978.

Sato, Shimada, T. T., Tanaka, M., Hayashi, T., and Watanabe, K., Formation of field-twisting flux tubes on the magnetopause and solar wind particle entry into the magnetosphere, *Geophys. Res. Lett.*, *13*, 801, 1986.

Schield, M. A., Freeman, J. W., and Dessler, A. J., A source for field-aligned currents at auroral latitudes, *J. Geophys. Res.*, *74*, 247–256, 1969.

Scholer, M., Magnetic flux transfer at the magnetopause based on single X line bursty reconnection, *Geophys. Res. Lett.*, *15*, 291, 1988.

Scholer, M., Models of flux transfer events, in *Physics of the Magnetopause, Geophys. Monogr. Ser.*, vol. 90, edited by P. Song, B. U. O. Sonnerup, and M. F. Thomsen, p. 235, AGU, Washington, D. C., 1995.

Scholer, M. and Treumann, R. A., The low-latitude boundary layer at the flanks of the magnetopause, *Space Sci. Rev.*, *80*, 341, 1997.

Sckopke, N., Paschmann, G., Haerendel, G., Sonnerup, B. U. O., Bame, S. J., Forbes, T. G., Hones, E. J., Jr., and Russell, C. T., Structure of the low-latitude boundary layer, *J. Geophys. Res.*, *86*, 2099, 1981.

Scudder, J. D., Theoretical approaches to the description of magnetic merging: The need for finite β_e, anisotropic ambipolar Hall MHD, *Space Sci. Rev.*, *80*, 235, 1997.

Shelley, E. G., Johnson, R. G., and Sharp, R. D., Satellite observations of energetic heavy ions during a geomagnetic storm, *J. Geophys. Res.*, *77*, 6104–6110, 1972.

Shelley, E. G., Sharp, R. D., and Johnson, R. G., Satellite observations of an ionospheric acceleration mechanism, *Geophys. Res. Lett.*, *3*, 654–656, 1976.

Shiokawa, K. and Yumoto, K., Global characteristics of particle precipitation and field-aligned electron acceleration during isolated substorms, *J. Geophys. Res.*, *98*, 1359–1375, 1993.

Shiokawa, K., Baumjohann, W., Haerendel, G., Paschmann, G., Fennel, J. F., Friis-Christensen, E., Luehr, H., Reeves, G. D., Russell, C. T., Sutcliffe, P. R., and Takahashi, K., High-speed ion flow, substorm current wedge, and multiple Pi2 pulsations, *J. Geophys. Res.*, *102*, in press, 1998.

Sibeck, D. G., Transient events in the outer magnetosphere: Boundary waves or flux transfer events?, *J. Geophys. Res.*, *97*, 4009, 1992.

Singer, H. J., Russell, C. T., Kivelson, M. G., Fritz, T. A., and Lennartsson, W., Satellite observations of the spatial extent and structure of Pc 3, 4, 5 pulsations near the magnetospheric equator, *Geophys. Res. Lett.*, *6*, 889–892, 1979.

Siscoe, G. L. and Maynard, N. C., Predicting substorms, in *Proceedings of the Third International Conference on Substorms (ICS-3)*, edited by E. J. Rolfe and B. Kaldeich, vol. SP-389, pp. 633–638, ESA, Noordwijk, 1996.

Smith, M. F. and Lockwood, M., The pulsating cusp, *Geophys. Res. Lett.*, *17*, 1069, 1990.

Smith, P. H., Bewtra, N. K., and Hoffman, R. A., Inference of the ring current ion composition by means of charge exchange decay, *J. Geophys. Res.*, *86*, 3470–3480, 1981.

Song, P. and Russell, C. T., Model of the formation of the low-latitude boundary layer for strongly northward interplanetary magnetic field, *J. Geophys. Res.*, *97*, 1411, 1992.

Sonnerup, B. U. O., Theory of the low-latitude boundary layer, *J. Geophys. Res.*, *85*, 2017–2026, 1980.

Sonnerup, B. U. O., Paschmann, G., and Phan, T.-D., Fluid aspects of reconnection at the magnetopause: In situ observations, in *Physics of the Magnetopause, Geophys. Monogr. Ser.*, vol. 90, edited by P. Song, B. U. O. Sonnerup, and M. F. Thomsen, p. 139, AGU, Washington, D. C., 1995.

Strangeway, R. J. and Johnson, R. G., Mass composition of substorm-related energetic ion dispersion events, *J. Geophys. Res.*, *88*, 2057–2064, 1983.

Strangeway, R. J. and Johnson, R. G., Energetic ion mass composition as observed at near-geosynchronous and low altitudes during the storm period of February 21 and 22, 1979, *J. Geo-*

phys. Res., *89*, 8919, 1984.

Swift, D. W., Effects of ion demagnetization in the plasma sheet, *J. Geophys. Res.*, *97*, 16,803–16,816, 1992.

Thorne, R. M. and Horne, R. B., Energy transfer between energetic ring current H^+ and O^+ by electromagnetic ion cyclotron waves, *J. Geophys. Res.*, *99*, 17,275–17,282, 1994.

Thorne, R. M. and Horne, R. B., Modulation of electromagnetic ion cyclotron instability due to interaction with ring current O^+ during magnetic storms, *J. Geophys. Res.*, *102*, 14,155–14,163, 1997.

Tinsley, B. A., Solar wind mechanism suggested for weather and climate change, *Eos Trans. AGU*, *75*, 369–374, 1994.

Treumann, R. A. and Bauer, T. M., Super-diffusion at the magnetopause, *Eos Trans. AGU*, *77* (46), Fall Meet. Suppl., 638, 1996.

Treumann, R. A., Labelle, J., and Pottelette, R., Plasma diffusion at the magnetopause: The case of lower hybrid drift waves, *J. Geophys. Res.*, *96*, 16009, 1991.

Tsurutani, B. T. and Gonzalez, W. D., The interplanetary causes of magnetic storms: A review, in *Magnetic Storms, Geophys. Monogr. Ser.*, vol. 98, edited by B. T. Tsurutani, W. D. Gonzalez, Y. Kamide, and J. K. Arballo, pp. 77–89, AGU, Washington, D. C., 1997.

Tsurutani, B. T. and Thorne, R. M., Diffusion processes at the magnetopause boundary layer, *Geophys. Res. Lett.*, *9*, 1247, 1982.

Tsurutani, B. T., Goldstein, B. E., Gonzalez, W. D., and Tang, F., Comment on "A new method of forecasting geomagnetic activity and proton showers" by A. Hewish and P. J. Duffet-Smith, *Planet. Space Sci.*, *36*, 205, 1988a.

Tsurutani, B. T., Gonzalez, W. D., Tang, F., Akasofu, S.-I., and Smith, E. J., Origin of interplanetary southward magnetic fields responsible for major magnetic storms near solar maximum (1978-1979), *J. Geophys. Res.*, *93*, 8519, 1988b.

Tsurutani, B. T., Brinca, A. L., Smith, E. J., andR. R. Anderson, R. T. O., and Eastman, T. E., A statistical study of ELF-VLF plasma waves at the magnetopause, *J. Geophys. Res.*, *94*, 1770, 1989.

Tsurutani, B. T., Gonzalez, W. D., Tang, F., and Lee, Y. T., Great magnetic storms, *Geophys. Res. Lett.*, *19*, 73–76, 1992.

Tsurutani, B. T., Arballo, J. K., Kamide, Y., Gonzalez, W. D., and Lepping, R. P., Interplanetary causes of great and superintense magnetic storms, *Phys. Chem. Earth*, this volume, 1998.

Valdivia, J. A., Sharma, A. S., and Papadopoulos, K., Prediction of magnetic storms by nonlinear models, *Geophys. Res. Lett.*, *23*(21), 2899–2902, 1996.

Vassiliadis, D., Klimas, A. J., Baker, D. N., and Roberts, D. A., A description of the solar wind-magnetosphere coupling based on nonlinear filters, *J. Geophys. Res.*, *100*, 3495–3512, 1995.

Vassiliadis, D., Angelopoulos, V., Baker, D. N., and Klimas, A. J., The relation between northern polar cap and auroral electrojet geomagnetic indices in the wintertime, *Geophys. Res. Lett.*, *23*, 2781–2784, 1996.

Viljanen, A. and Pirjola, R., Finnish geomagnetically induced currents project, *IEEE Power Engineering Review*, *15*, 20–21, 1995.

von Steiger, R., *Composition of the solar wind*, Habilitation Thesis, Univ. of Bern, Switzerland, 1995.

von Steiger, R., Geiss, J., Gloeckler, G., Balsiger, H., Galvin, A. B., Mall, U., and Wilken, B., Magnesium, carbon and oxygen abundances in different solar wind flow types as measured by SWICS on Ulysses, in *Solar Wind Seven*, edited by E. Marsch and R. Schwenn, pp. 399–404, Pergamon Press, London, 1992.

von Steiger, R., Geiss, J., and Gloeckler, G., Composition of the solar wind, in *Cosmic Winds and the Heliosphere*, edited by J. R. Jokipii, C. P. Sonett, and M. S. Giampapa, Univ. of Arizona Press, Tucson, AZ, in press, 1997.

Watanabe, Y., Hillman, D. C., Otsuka, K., Bingham, C., Breus, T. K., Cornélissen, G., and Halberg, F., Cross-spectral coherence between geomagnetic disturbance and human cardiovascular variables at non-societal frequencies, *Chronobiologia*, *21*, 265–272, 1994.

Weimer, D. R., A flexible, IMF-dependent model of high-latitude electric potentials having "space weather" applications, *Geophys. Res. Lett.*, *23*, 2549–2552, 1996.

Whipple Jr., E. C., (UBK) co-ordinates: a natural system for studying magnetospheric convection, *J. Geophys. Res.*, *83*, 4318, 1978.

Wilken, B., Weiß, W., Hall, D., Grande, M., Søraas, F., and Fennell, J. F., Magnetospheric Ion Composition Spectrometer onboard the CRRES spacecraft, *J. of Spacecraft and Rockets*, *29*, 585–591, 1992.

Wilken, B., Daglis, I. A., Milillo, A., Orsini, S., Doke, T., Livi, S., and Ullaland, S., Energetic neutral atoms in the outer magnetosphere: An upper flux limit obtained with the HEP-LD spectrometer on board GEOTAIL, *Geophys. Res. Lett.*, *24*, 111–114, 1997.

Williams, D. J., The Earth's ring current: Causes, generation, and decay, *Space Sci. Rev.*, *34*, 223–234, 1983.

Williams, D. J., Roelof, E. C., and Mitchell, D. G., Global magnetospheric imaging, *Rev. Geophys.*, *30*, 183–208, 1992.

Wimmer, R. F., Schweingruber, R., von Steiger, R., and Paerli, R., Solar wind stream interfaces in corotating interaction regions: SWICS/Ulysses results, *J. Geophys. Res.*, in press, 1997.

Wolf, R. A., J. W. Freeman Jr., Hausmann, B. A., Spiro, R. W., Hilmer, R. V., and Lambour, R. L., Modeling convection effects in magnetic storms, in *Magnetic Storms, Geophys. Monogr. Ser.*, vol. 98, edited by B. T. Tsurutani, W. D. Gonzalez, Y. Kamide, and J. K. Arballo, vol. 39, pp. 161–172, AGU, Washington, D. C., 1991.

Wray, J. and Green, G. G. R., Calculation of the Volterra kernels of nonlinear dynamic systems using an artificial neural network, *Biological Cybernetics*, *71*, 187, 1994.

Wu, J.-G. and Lundstedt, H., Prediction of geomagnetic storms from solar wind data using Elman recurrent neural networks, *Geophys. Res. Lett.*, *23*, 319, 1996.

Yau, A. W., Whalen, B. A., Peterson, W. K., and Shelley, E. G., Distribution of upflowing ionospheric ions in the high-altitude polar cap and auroral ionosphere, *J. Geophys. Res.*, *89*, 5507–5522, 1984.

Young, D. T., Perraut, S., Roux, A., C. de Villedary, Gendrin, R., Korth, A., Kremser, G., and Jones, D., Wave-particle interactions near Ω_{He+} observed on GEOS 1 and 2: 1. Propagation of ion cyclotron waves in He^+-rich plasma, *J. Geophys. Res.*, *86*, 6755–6772, 1981.

Young, D. T., Balsiger, H., and Geiss, J., Correlations of magnetospheric ion composition with geomagnetic and solar activity, *J. Geophys. Res.*, *87*, 9077–9096, 1982.